# Reliability of a nonlinear fluctuation-dissipation relation as a test of Markovianity

Georg Podhaisky,[1,2,*] Igor M. Sokolov,[2] Yael Roichman,[3,4] and Benjamin Lindner[1,2]

[1] *Bernstein Center for Computational Neuroscience Berlin, Philippstr. 13, Haus 6, 10115 Berlin, Germany*
[2] *Physics Department of Humboldt University Berlin, Newtonstr. 15, 12489 Berlin, Germany*
[3] *The Raymond and Beverley School of Physics and Astronomy, Tel Aviv University, Tel Aviv 6997801, Israel*
[4] *The Raymond and Beverley School of Chemistry, Tel Aviv University, Tel Aviv 6997801, Israel*

(Received 12 December 2025; accepted 30 March 2026; published 23 April 2026)

Markov processes are widely applied in modeling random phenomena, and the corresponding models can be analyzed within an established theoretical framework. It is thus desirable to have reliable tests for the (non-)Markovianity of a physical or biological system at hand. One such test, suggested by Engbring *et al.* [Phys. Rev. X **13**, 021034 (2023)], is based on a nonlinear fluctuation-dissipation relation (NL-FDR) that compares spontaneous fluctuations with the response to (nonweak) external perturbations. A violation of this NL-FDR indicates non-Markovianity. However, estimating the relevant statistics for the variable conjugated to the perturbation from finite experimental data can be challenging. Comparing noisy estimates of the spontaneous and the response statistics can lead to apparent deviations from the prediction of the NL-FDR. So, when is a violation of the NL-FDR due to non-Markovian features of the system and when is it due to a finite sample size? We consider this question for the simplest Markovian example, the overdamped harmonic oscillator with thermal white noise and subject to a constant force perturbation. We derive analytical expressions for the variances of the estimators for the spontaneous correlation function and for the time-dependent mean response. We confirm previous findings that there is an optimal amplitude for the perturbation at which the test of non-Markovianity is most reliable. In terms of the original variable, the optimal amplitude is such that the response to the perturbation is of the order of one standard deviation of the spontaneous fluctuations. Put differently, the optimal amplitude neither corresponds to the linear-response regime of very weak perturbations nor to the regime of very strong perturbations where the response is largely deterministic. At large amplitudes, we encounter heavy-tailed distributions of certain estimators, which we discuss.

DOI: 10.1103/485b-sb1x

## I. INTRODUCTION

Markov processes form an important class of stochastic models for time series that are shaped by randomness. A Markov process $x(t)$ is defined by the property that the conditional probability density of being at $x_{n+1}$ at time $t_{n+1}$ if the process has been at $x_n$ at time $t_n < t_{n+1}$, at $x_{n-1}$ at time $t_{n-1} < t_n$, etc. depends only on the timewise last condition:

$$P(x_{n+1}, t_{n+1}|x_n, t_n; x_{n-1}, t_{n-1}; \dots) = P(x_{n+1}, t_{n+1}|x_n, t_n). \tag{1}$$

Put differently, the future of a Markov process is only determined by its present state, not by its past. It is completely determined by its transition probability (the right-hand side in the above equation), which can be found by (comparatively simple) Fokker-Planck or master equations that are local in time (see standard textbooks [1–3]). As pointed out by Engbring *et al.* [4], the development of a mathematical description of stochastic systems outside of equilibrium therefore requires a procedure to differentiate between Markov and non-Markov systems. The ability to detect non-Markovianity is also useful for identifying the relevant stochastic variables for the description of a given system [5,6]: Lower-dimensional non-Markovian models of physical systems often appear by considering only a subset of variables of a higher-dimensional Markov system and projecting out irrelevant, i.e., noninteresting variables, as illustrated in Ref. [7] (pp. 19 therein) and rigorously discussed in Ref. [8]. Thus, the original question by Onsager and Machlup arises of how to determine whether a given set of variables suffices for a Markovian description [9].

There are different approaches to investigate whether a given system is Markovian. First, it has been proposed to analyze the corresponding time series. The direct method is to check the fulfillment of the Chapman-Kolmogorov equation [10]. Other approaches rely on certain properties related to Markovianity, such as transition path probabilities [11], the distribution of transition path times [6], or the entropy rate in the case of a discrete state space [12].

An alternative strategy to test for Markovianity of physical systems that can be externally perturbed is based on generalized fluctuation-dissipation relations (FDRs) that describe the connection of the fluctuations of an unperturbed nonequilibrium system to how it reacts if perturbed by an external force [4,5,13]. If such a relation is derived under the assumption of

*Contact author: georg.podhaisky@physik.hu-berlin.de

Markovianity, its violation can be used to infer that the system is non-Markovian [4,5]. This concept was demonstrated for a linear nonequilibrium FDR in Ref. [5], which showed that for the respective sample system it is difficult to distinguish whether violations of the FDR are linked to non-Markovianity or whether they are solely due to measurement effects, such as estimating statistics from a limited ensemble or a violation of the linear response ansatz by finite perturbation amplitudes. This analysis led to the conclusion that a reliable detection of non-Markovianity might only be possible if a large amount of data is accessible [5]. To be able to assess the Markovianity of systems for which fewer experimental data exist, it was proposed in Ref. [4] to use a nonlinear generalized fluctuation-dissipation relation (NL-FDR) which is applicable to stronger perturbations. The authors argued that larger perturbation amplitudes evoke more pronounced response signals, which lead to an improved estimation of the corresponding statistics at a small ensemble of realizations and thus a better test of Markovianity [4]. The NL-FDR derived in [4],

$$\langle z^{(\mathrm{tr})}(\tau)\rangle = C_z(\tau), \tag{2}$$

relates the correlation function of the variable $z(t)$ in the unperturbed state, $C_z(\tau)$, to the mean transient response $\langle z^{(\mathrm{tr})}(\tau)\rangle$ of the same variable $z(t)$ after a constant perturbation has been switched off. The variable for which this relation holds true, $z(t) \equiv z(x(t))$, is defined by

$$z(x) \equiv \frac{P_\varepsilon(x)}{P_0(x)} - 1. \tag{3}$$

Here, the perturbed and unperturbed steady-state distributions $P_\varepsilon(x)$ and $P_0(x)$, respectively, have been used [4]. The variable $z(x)$ is conjugated to the specific perturbation applied to the system.

As in Ref. [5], the authors of Ref. [4] used a finite ensemble to estimate the statistics leading to apparent deviations from the NL-FDR even in the case of a Markovian system where it holds true analytically. It is apparent from Ref. [4] that since such a deviation is supposed to be used as an indication of non-Markovianity, this measurement effect is the limiting factor in the reliability of the testing procedure. The authors observed that the deviation is minimal at intermediate perturbation amplitudes and they provided qualitative arguments to explain the existence of a minimum: At intermediate perturbations, the response is set apart from the noise level to a higher degree and $z(x)$ maps to a larger interval than for small perturbations but the outer tails of the distributions do not enter the transformation $z(x)$ as would be the case for even larger amplitudes [4]. However, they did not provide a quantitative discussion of the measurement effects.

For an optimal testing procedure working well with limited data, these finite-size effects must be minimized by the proper choice of the perturbation amplitude. Quantitative expressions for the measurement uncertainty of the statistical estimators in the NL-FDR are a prerequisite for this optimization.

In addition, these quantitative expressions provide a metric for assessing the significance of an observed NL-FDR deviation, allowing one to decide if the deviation stems from statistical fluctuations or genuinely indicates non-Markovianity. The present work, therefore, aims at quantifying the uncertainty of the statistics $C_z(\tau)$ and $\langle z^{(\mathrm{tr})}(\tau)\rangle$ if they are estimated from a finite ensemble. Specifically, we choose the analytically tractable Ornstein-Uhlenbeck process with a step perturbation in the mean. We emphasize that the variable $z(x)$ given by Eq. (3) and conjugated to the perturbation of this linear process shows a nonlinear response to such a perturbation. For other applications of linear stochastic processes to study irreversibility and memory, see, e.g., Refs. [14,15].

The problem of quantifying the uncertainty of different statistical estimators has been extensively studied in the theory of time series analysis. For the autoregressive process of order one [AR(1)], which is a temporally discrete version of the Ornstein-Uhlenbeck process [16] and generalizations thereof, several results have been derived for estimators in the original variable $x$ [17,18]. Our problem, the variance of the empirical transient mean and empirical stationary correlation of a nonlinear transformation $z(x)$ of a Gaussian process, has not been addressed to the best of our knowledge.

Our main result confirms the intuition about the existence of an optimal intermediate perturbation amplitude. This holds even if we neglect one source of error in determining the conjugated variable according to Eq. (3) for strong perturbations: Its large random errors due to little overlap between the estimators of the stationary probability densities $P_0(x)$ and $P_\varepsilon(x)$. For our example of the Ornstein-Uhlenbeck process, we know the conjugated variable exactly [4], and we can focus on the sources of statistical uncertainty that are unrelated to the estimation of the conjugated variable, $z(x)$ Eq. (3), itself. Our results indicate that a very strong uncertainty about the equality of the left- and right-hand sides of the NL-FDR Eq. (2) is encountered for perturbation amplitudes that induce deviations of the mean beyond one standard deviation of stationary fluctuations. To test the Markovianity of the system, it pays off to choose amplitudes that provoke a response beyond the pure linear-response regime, inducing changes of the order of one standard deviation. However, a further increase of the amplitude leading into a strongly nonlinear-response regime drastically boosts the statistical uncertainty in the quantities connected by the NL-FDR. Hence, to test the Markovianity of a given system, it is recommended to choose a perturbation amplitude close to the onset of the nonlinear-response regime, a conclusion that most likely also applies to a broader class of systems.

The paper is structured as follows: We first introduce our model and statistics of interest and recall the test protocol from Ref. [4] in Sec. II. To set the stage, we then revisit the problem of the correlation estimator in the original variable $x$ of the Ornstein-Uhlenbeck process in Sec. III A. In Secs. III B and III C, the variances of the estimators of the mean transient and the correlation of the conjugated variable $z$ are derived. Their combined variance is discussed in Sec. III D. We conclude with a summary of our results and point out open questions for further investigation in Sec. IV.

## II. MODEL, STATISTICS, AND TEST PROTOCOL

The statistical properties of the fluctuation-dissipation relation are derived for an Ornstein-Uhlenbeck process that is defined by the Langevin equation

$$\dot{x} = -\kappa[x(t) - \varepsilon\,\Theta(T/2 - t)] + \sqrt{2D}\xi(t), \tag{4}$$

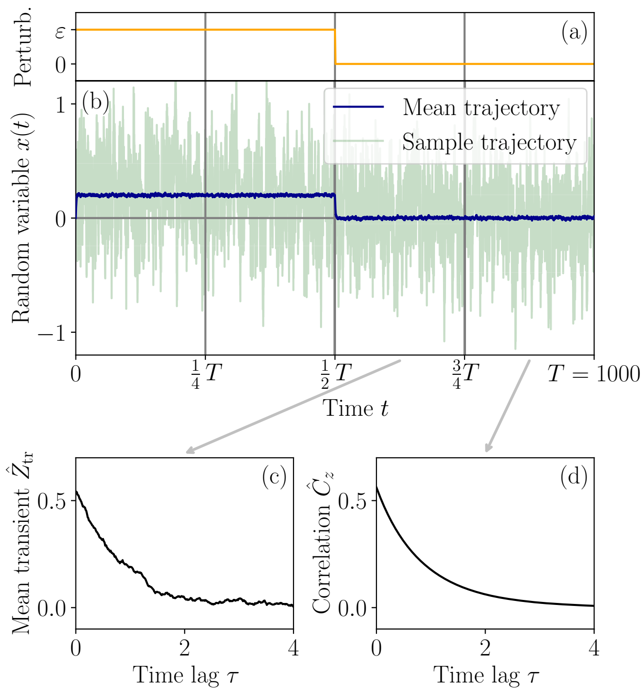


FIG. 1. Measurement protocol [4] for an Ornstein-Uhlenbeck process described by Eq. (4) with $N = 2000$ realizations. The parameters $D = 1/11$, $\kappa = 1$, $\varepsilon = 0.2$, $T = 1000$, and the simulation timestep $\Delta t = 0.01$ are chosen in accordance with Ref. [4]. The perturbation $\varepsilon\,\Theta(T/2 - t)$ in (a) causes the response of the system shown in (b). This response is measured in terms of transient trajectories $\{x_i^{(\rm tr)}(\tau)\}$ in $[T/2, 3T/4]$ which are used to calculate the estimator of the mean transient response $\hat{Z}_{\rm tr}$ in (c). The steady-state trajectories $\{x_i(\tau)\}$ in $[3T/4, T]$ are used to calculate the correlation estimator $\hat{C}_z$ in (d). The transformation to the conjugated variable $x \to z(x)$ is carried out with the exact expression of $z(x)$ instead of measured distributions.

with white Gaussian noise $\langle \xi(t)\xi(t')\rangle = \delta(t - t')$ and a time-dependent perturbation $\varepsilon\,\Theta(T/2 - t)$, which was used in Ref. [4] as a simple example for a Markovian system.

The following measurement protocol for collecting all necessary data from a given stochastic process was proposed in Ref. [4] and is depicted in Fig. 1: A total of $N$ independent trajectories is recorded, each for a time interval of length $T$ in which the perturbation is switched on during $t \in [0, T/2]$ and switched off during $t \in [T/2, T]$. For a sufficiently large time $T$, the process can be approximated to be in its perturbed steady state by $t = T/4$ after being initialized at $t = 0$. During $t \in [T/4, T/2]$, the corresponding distribution $P_\varepsilon(x)$ is measured. The system's response to switching off the perturbation, i.e., the set of transient trajectories $\{x_i^{(\rm tr)}(\tau)\}$ with $i = 1, \ldots, N$, is then recorded during $t \in [T/2, 3T/4]$, where $\tau = 0$ is chosen at $T/2$. As before, it is assumed that the system is in its unperturbed steady state by $t = 3T/4$. Finally, the last quarter $t \in [3T/4, T]$ is used to measure the unperturbed steady-state distribution $P_0(x)$ and to record steady-state trajectories $\{x_i(\tau)\}$ with $i = 1, \ldots, N$ and $\tau = 0$ at $3T/4$.

In Ref. [4], the conjugated variable $z(x) = P_\varepsilon(x)/P_0(x) - 1$ was then calculated with the measured distributions and used to transform the trajectories as $z(t) \equiv z(x(t))$. In the notation introduced above, this results in a set of transient trajectories of the conjugated variable (conjugate) $\{z_i^{(\rm tr)}(\tau)\}$ and steady-state trajectories of the conjugate, $\{z_i(\tau)\}$.

Finally, the former set of trajectories is used to calculate the statistical estimator

$$\tilde{Z}_{\rm tr}(\tau) \equiv \frac{1}{N}\sum_{i=1}^{N} z_i^{(\rm tr)}(\tau), \tag{5}$$

which approximates the mean transient response $\tilde{Z}_{\rm tr}(\tau) \approx \langle z_i^{(\rm tr)}(\tau)\rangle$ and the latter set is used to determine the estimator

$$\tilde{C}_z(\tau) \equiv \frac{1}{N}\frac{1}{T/4 - \tau}\sum_{i=1}^{N}\int_0^{T/4-\tau} z_i(t) z_i(t+\tau)\,dt, \tag{6}$$

which approximates the autocorrelation function in the new variable $\tilde{C}_z(\tau) \approx C_z(\tau) = \langle z_i(0) z_i(\tau)\rangle$ [4]. In the following, the estimators of the mean transient response and the correlation function are also referred to as empirical mean transient response and empirical correlation function.

When aiming for a description of the statistical uncertainty of the fluctuation-dissipation relation, two sources of stochasticity are relevant:

(1) The statistical estimators $\tilde{C}_z$ and $\tilde{Z}_{\rm tr}$, which enter the NL-FDR Eq. (2), are calculated from a finite ensemble of realizations of the stochastic process. Thus, they show stochastic deviations from the corresponding true statistics.

(2) The mapping to the conjugated variable $x \to z(x) = P_\varepsilon(x)/P_0(x) - 1$ is determined by the distributions of the stochastic process. If these distributions stem from measured histograms, their stochastic deviations from the exact distributions enter the calculation and result in a stochastic map $\hat{z}(x)$ that may significantly differ from the true conjugated variable $z(x)$.

The present work analyses the first of these contributions and assumes an exact and deterministic map $z(x)$ for simplicity (for a brief comparison of the two contributions, see Sec. IV). To compare the resulting predictions to simulation results, the above simulation protocol is modified accordingly. Instead of measuring histograms for the probability distributions $P_\varepsilon(x)$ and $P_0(x)$, the corresponding exact expressions are used in the calculation of the conjugated variable $z(x) = P_\varepsilon(x)/P_0(x) - 1$. Specifically, for the Ornstein-Uhlenbeck process, the conjugated variable takes the form [4]

$$z(x) = \exp\left(\frac{-\varepsilon^2}{2\sigma_x^2} + \frac{\varepsilon\, x}{\sigma_x^2}\right) - 1, \tag{7}$$

with $\sigma_x^2 = D/\kappa$. We note for later use that the variable $z$ obeys a generalized log-normal distribution (because $x$ is normally distributed). This implies, especially for large values of $\varepsilon$, a fat tail of the stationary distribution of $z$.

All numerical results presented in this work are obtained from a simulation of the Ornstein-Uhlenbeck process Eq. (4) in accordance with this modified protocol. The simulation is carried out using the Euler-Maruyama integration scheme with a time step of $\Delta t = 0.01$. It results in two data sets $\{x_{i,k}\}$ and $\{x_{i,k}^{(\rm tr)}\}$, where $i = 1, \ldots, N$ is the realization index and $k = 0, \ldots, N_T - 1$ denotes the time index. As before, $\{x_{i,k}^{(\rm tr)}\}$ is the set of transient trajectories with $k = 0$ at $T/2$ and $\{x_{i,k}\}$ denotes the set of steady-state trajectories with $k = 0$ at $3T/4$. The trajectories in the original variable $x_{i,k}$ are converted to trajectories in the conjugated variable $z_{i,k}$ by inserting them into Eq. (7), i.e., $z_{i,k} = z(x_{i,k})$ and $z^{(\mathrm{tr})}_{i,k} = z(x^{(\mathrm{tr})}_{i,k})$.

The correlation function $C_z(\tau) = \langle z(0)z(\tau)\rangle$ at $\tau = n\,\Delta t$ is estimated from simulated data by a mixed ensemble and time average

$$\hat{C}_z(n) \equiv \frac{1}{N(N_T - n)} \sum_{i=1}^{N} \sum_{k=0}^{N_T-1-n} z_{i,k} z_{i,k+n}, \tag{8}$$

which is the discretization of the estimator Eq. (6). The correlation estimator $\hat{C}_x(n) \approx C_x(n\Delta t)$ of the original variable $x(t)$ is also discussed below as an introductory example. It is given by

$$\hat{C}_x(n) \equiv \frac{1}{N(N_T - n)} \sum_{i=1}^{N} \sum_{k=0}^{N_T-1-n} x_{i,k}\, x_{i,k+n}. \tag{9}$$

For both correlation estimators, the time index is restricted to $n = 0, \ldots, N_T - 1$. The empirical mean transient response in the conjugated variable $z^{(\mathrm{tr})}(\tau)$ at $\tau = n\,\Delta t$ follows directly from the corresponding expression for continuous trajectories Eq. (5):

$$\hat{Z}_{\mathrm{tr}}(n) \equiv \frac{1}{N} \sum_{i=1}^{N} z^{(\mathrm{tr})}_{i,n}. \tag{10}$$

The analytical expressions for the corresponding exact statistics are stated in [4]

$$C_x(\tau) = \langle x_i(0)x_i(\tau)\rangle = \sigma_x^2 e^{-\kappa|\tau|}, \tag{11}$$

$$C_z(\tau) = \langle z_i(0)z_i(\tau)\rangle = \exp\left(\frac{\varepsilon^2}{\sigma_x^2} e^{-\kappa|\tau|}\right) - 1, \tag{12}$$

$$\left\langle z^{(\mathrm{tr})}_i(\tau)\right\rangle = \exp\left(\frac{\varepsilon^2}{\sigma_x^2} e^{-\kappa|\tau|}\right) - 1. \tag{13}$$

Since both $\langle z_i(\tau)\rangle$ and $\langle x_i(\tau)\rangle$ vanish in the unperturbed steady state [4], the definition of the correlation function $C_y(\tau) = \langle y(0)y(\tau)\rangle$ coincides with the autocovariance $\langle y(0)y(\tau)\rangle - \langle y(0)\rangle\langle y(\tau)\rangle$ for $y \in \{x_i, z_i\}$ in the time interval $t \in [3T/4, T]$.

## III. RESULTS

### A. Uncertainty of the correlation estimator in the original variable $x$

As a first approach to the problem, the properties of the correlation estimator

$$\hat{C}_x(n) = \frac{1}{N(N_T - n)} \sum_{i=1}^{N} \sum_{k=0}^{N_T-1-n} x_{i,k} x_{i,k+n} \tag{14}$$

in the original variable $x$ of the Ornstein-Uhlenbeck process are analyzed. As stated before, the data of the unperturbed process in its steady state is used, i.e., the data $\{x_{i,k}\}$ is recorded during $t \in [3T/4, T]$. In the following analysis, the moments of $\hat{C}_x$ are rewritten in terms of moments of $x$, which are presented in Appendix A.

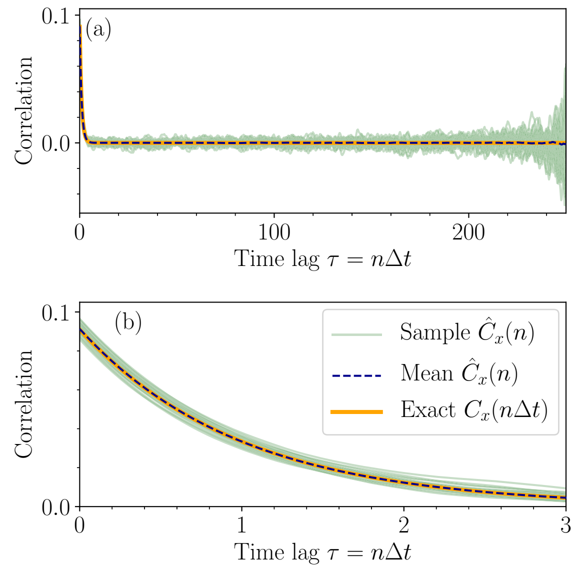


FIG. 2. Correlation function of the original variable $x$ depicted over two time intervals, [0,250] in (a) and [0,3] in (b). The analytical expression Eq. (11) (orange) is compared to 31 correlation estimators (green) and to the mean over 1000 estimators (blue), which are calculated for distinct ensembles. Each of those ensembles contains $N = 10$ simulated trajectories, each of length $N_T = 25\,001$ at $\Delta t = 0.01$, which corresponds to $T = 1000$ in the measurement protocol. The other parameters are $D = 1/11$ and $\kappa = 1$.

The estimator's first moment is given by

$$\begin{aligned}\langle\hat{C}_x(n)\rangle &= \frac{1}{N(N_T - n)} \sum_{i=0}^{N} \sum_{k=0}^{N_T-1-n} \langle x_{i,k}x_{i,k+n}\rangle \\ &= \frac{1}{N(N_T - n)} \sum_{i=1}^{N} \sum_{k=0}^{N_T-1-n} C_x(n\Delta t) \\ &= C_x(n\Delta t).\end{aligned} \tag{15}$$

This shows that the estimator is unbiased as it averages at the exact correlation function. For a single trajectory estimator, i.e. $N = 1$, this is a well-known fact, see [19] (p. 73 therein, if applied to a process with vanishing mean) or [20] (p. 162 therein, also mentioning ergodicity as a condition). This is consistent with simulation results. Figure 2 shows that the empirical mean of 1000 correlation estimators $\hat{C}_x$ coincides with the exact correlation function $C_x$. The trajectories are obtained by following the measurement protocol from Sec. I and leaving out the mapping to the conjugated variable $x \to z(x)$.

The calculation of the variance of $\hat{C}_x$ can be simplified as all trajectories are independent. The ensemble average simply results in a prefactor $1/N$ [21] (p. 110 therein) and thus follows:

$$\begin{aligned}\mathrm{Var}\big(\hat{C}_x(n)\big) &= \frac{1}{N}\mathrm{Var}\left(\frac{1}{(N_T - n)} \sum_{k=0}^{N_T-1-n} x_{i,k}x_{i,k+n}\right) \\ &= \frac{1}{N(N_T - n)^2} \sum_{k,l=0}^{N_T-1-n} \langle x_{i,k}x_{i,k+n}x_{i,l}x_{i,l+n}\rangle \\ &\quad - \frac{1}{N}\{C_x[n\Delta t]\}^2.\end{aligned} \tag{16}$$

In the second line, the variance is written in terms of moments and the exact correlation function $C_x$ is identified in the second term. The fourth moment presented in Appendix A is inserted and the double sum is simplified, see Appendix B. This results in

$$\mathrm{Var}(\hat{C}_x(n)) = \frac{1}{N(N_T-n)^2} \sum_{k=-(N_T-n-1)}^{N_T-n-1} (N_T - n - |k|) \times (\{C_x[k\Delta t]\}^2 + C_x[(n+k)\Delta t] C_x[(n-k)\Delta t]). \tag{17}$$

A very similar derivation for the covariance of the estimator is stated in [18] (p. 226 therein) for a class of processes that includes the autoregressive process of order one [AR(1)] [18] (example 3.2.2. therein after setting $\psi_j = 0$ for negative $j$). If the autocovariance function in the corresponding expression in [18] is replaced by the correlation function of the Ornstein-Uhlenbeck process and the fourth moment of the white Gaussian noise is inserted, the above expression can be read off as a special case of the covariance with the additional restriction to single trajectories, i.e. $N = 1$.

The result Eq. (17) can be simplified further. For details, see Appendix B. The final expression for the variance of the correlation estimator of $x(t)$ reads

$$\begin{aligned}\mathrm{Var}(\hat{C}_x(n)) &= \frac{\sigma_x^4}{N(N_T-n)^2}\Big\{(N_T-n)(-r^n-1+2r^n n) - r^n(n-1)n \\ &\quad + \frac{2}{(1-r)^2}[(N_T-n)(1-r) - r + 2r^{N_T-n+1} \\ &\quad + (N_T-2n)r^n - (N_T-2n+1)r^{n+1}]\Big\},\end{aligned} \tag{18}$$

where $r \equiv e^{-2\kappa\Delta t}$. In the course of the calculation, the time index was restricted to $n \leqslant (N_T-1)/2$ to simplify the expression. For the closely related case of an AR(1) process, Ref. [17] includes an approximate expression for $\mathrm{Var}(\hat{C}_x(n))$ which disregards terms of order $O(1/(N_T-n)^2)$. This result is consistent with the above exact expression if the correlation function of the AR(1) process is replaced by the correlation function of the Ornstein-Uhlenbeck process. This is shown in Appendix B.

The validity of Eq. (18) is tested with simulation results. The corresponding prediction of the standard deviation

$$\Delta\hat{C}_x = \sqrt{\mathrm{Var}(\hat{C}_x)} \tag{19}$$

shows good agreement with the measured standard deviation of correlation estimators of independent ensembles; see Fig. 3.

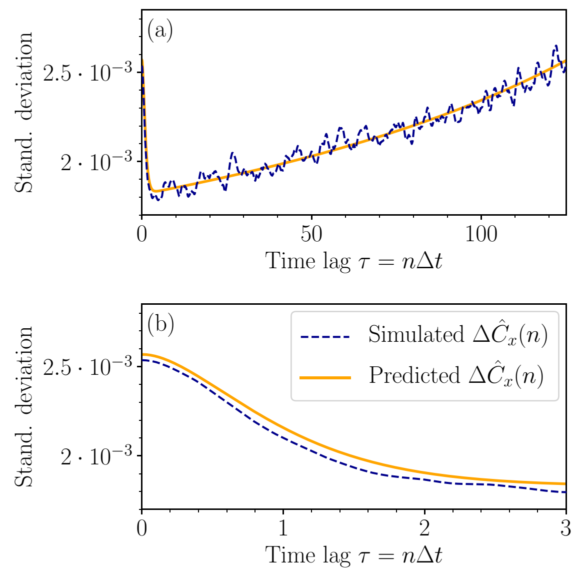


FIG. 3. Standard deviation of the correlation estimator of the variable $x$ depicted over two time intervals, [0,125] in (a) and [0,3] in (b). The analytical expression of the standard deviation obtained from Eq. (18) (orange) is compared to the measured standard deviation of 1000 correlation estimators (blue), which are calculated for distinct ensembles. Each of those ensembles contains $N = 10$ trajectories simulated for $N_T = 25\,001$ at $\Delta t = 0.01$, i.e., $T = 1000$ in the protocol, and with parameters $D = 1/11$ and $\kappa = 1$.

### B. Uncertainty of the correlation estimator in the conjugated variable $z$

The correlation estimator in the conjugated variable $\hat{C}_z$ is analyzed in terms of its average and variance. By replacing the original variable $x$ by the conjugated variable $z$ in Eq. (15), it is obvious that also $\hat{C}_z$ is an unbiased estimator. As before, this prediction is confirmed by the simulation results. The agreement of the mean of the correlation estimators and the exact correlation function $C_z$ is shown in Fig. 4.

We calculate the variance of the correlation estimator, treating it as a special case of the covariance $\mathrm{Cov}(\hat{C}_z(n), \hat{C}_z(m))$. The latter covariance will be needed in any case in the further analysis in Appendix D. As before, the covariance calculation for the estimator of multiple independent trajectories can be reduced to the case of a single trajectory by introducing a prefactor $1/N$:

$$\begin{aligned}\mathrm{Cov}(\hat{C}_z(n), \hat{C}_z(m)) &= \frac{1}{N}\mathrm{Cov}\Bigg(\frac{1}{(N_T-n)}\sum_{l=0}^{N_T-1-n} z_{i,l}z_{i,l+n}, \\ &\qquad \frac{1}{(N_T-m)}\sum_{k=0}^{N_T-1-m} z_{i,k}z_{i,k+m}\Bigg) \\ &= \frac{1}{N}\Bigg\{\Bigg[\frac{1}{(N_T-n)(N_T-m)}\sum_{l=0}^{N_T-1-n}\sum_{k=0}^{N_T-1-m} \\ &\quad \times \langle z_{i,l}z_{i,l+n}z_{i,k}z_{i,k+m}\rangle\Bigg] - C_z(n\Delta t)C_z(m\Delta t)\Bigg\}.\end{aligned} \tag{20}$$

As before, the definition of the covariance in terms of second and first moments is used in the second line and the exact correlation function $C_z$ is identified. Inserting the fourth moment, which is calculated in Appendix A, and substituting summation indices yields a lengthy expression for the covariance, see Eq. (C4). Evaluating this expression at $n = m$ finally results in the following expression for the variance of the correlation

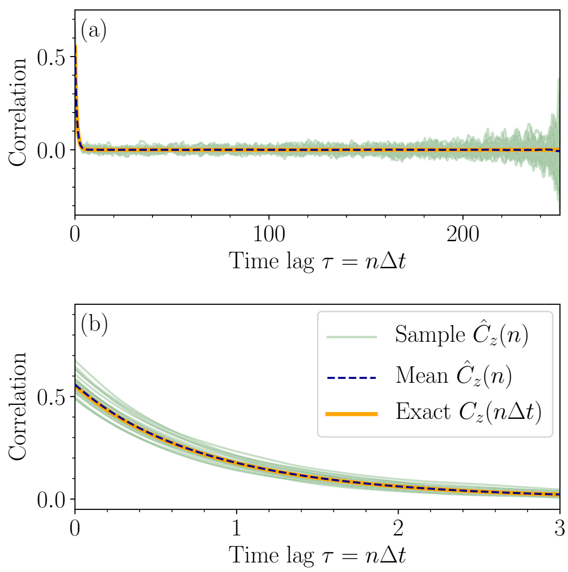


FIG. 4. Correlation function of the conjugated variable $z$ depicted over two time intervals, [0,250] in (a) and [0,3] in (b). The analytical expression Eq. (12) (orange) is compared to 31 correlation estimators (green) and to the mean over 1000 estimators (blue), which are calculated for distinct ensembles. Each of those ensembles contains $N = 10$ simulated trajectories, each of length $N_T = 25\,001$ at $\Delta t = 0.01$, i.e., $T = 1000$. The other parameters are $D = 1/11$, $\kappa = 1$, and $\varepsilon = 0.2$.

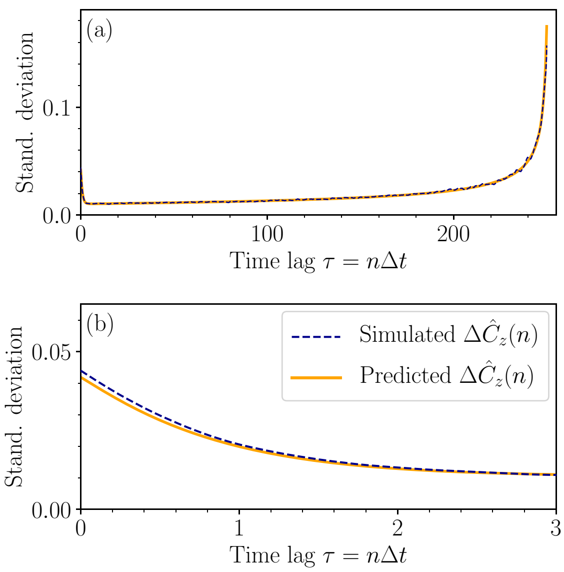


FIG. 5. Standard deviation of the correlation estimator of the conjugated variable depicted over two time intervals, [0,250] in (a) and [0,3] in (b). The analytical expression obtained as the square root of Eq. (C4) (orange) is compared to the measured standard deviation of 1000 correlation estimators (blue), which are calculated for distinct ensembles. Each of those ensembles contains $N = 10$ simulated trajectories, each of length $N_T = 25\,001$ at $\Delta t = 0.01$, i.e., $T = 1000$. The other parameters are $D = 1/11$, $\kappa = 1$, and $\varepsilon = 0.2$.

estimator of $z(t)$:

$$\begin{aligned}
&\mathrm{Var}\big(\hat{C}_z(n)\big)\\
&\quad= -\frac{1}{N}[C_z(n\Delta t) - 1]^2 + \frac{1}{N(N_T - n)}\big[2e^{f(0)} + 2e^{f(n)}\\
&\qquad - 4e^{f(0)+2f(n)} + e^{2f(0)+4f(n)}\big]\\
&\qquad + \frac{2}{N(N_T - n)^2}\sum_{k=1}^{N_T-n-1}\big\{(N_T - n - k)\big[2e^{f(k)}\\
&\qquad + e^{f(|n-k|)} + e^{f(k+n)} + e^{2f(n)+2f(k)+f(|-k+n|)+f(k+n)}\\
&\qquad - 2e^{f(n)+f(k)+f(k+n)} - 2e^{f(n)+f(k)+f(|-k+n|)}\big]\big\},
\end{aligned} \tag{21}$$

with $f(j) = e^{-\kappa j \Delta t}\varepsilon^2/\sigma_x^2$. The detailed derivation is presented in Appendix C. The corresponding standard deviation

$$\Delta\hat{C}_z(n) = \sqrt{\mathrm{Var}(\hat{C}_z(n))} \tag{22}$$

is compared to the empirical standard deviation of 1000 independent realizations of the correlation estimator. For simplicity, the computation of the predicted variance is done directly with Eq. (C4), evaluated at $n = m$.

As shown in Fig. 5, the prediction agrees with the simulation results.

### C. Uncertainty of the empirical mean transient response in the conjugated variable $z$

The estimator of the mean transient response

$$\hat{Z}_{\mathrm{tr}}(n) = \frac{1}{N}\sum_{i=1}^{N} z_{i,n}^{(\mathrm{tr})} \tag{23}$$

is unbiased, i.e., $\langle \hat{Z}_{\mathrm{tr}}(n)\rangle = \langle z_i^{(\mathrm{tr})}(n\Delta t)\rangle$. This can be easily seen by pulling the averaging operation into the sum. This is also observed in the simulation. Figure 6 shows good agreement of the empirical mean transient response averaged over

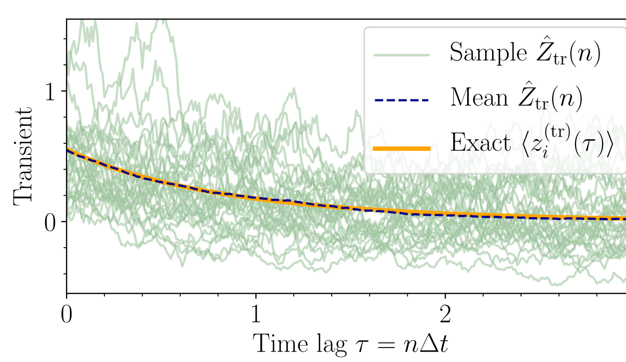


FIG. 6. The analytical expression of the averaged transient response Eq. (13) (orange) is compared to 31 estimators $\hat{Z}_{\mathrm{tr}}(n)$ (green) and to the mean over 1000 estimators (blue), which are calculated for distinct ensembles. Each of the ensembles contains $N = 10$ trajectories simulated with $D = 1/11$, $\kappa = 1$ and $\varepsilon = 0.2$, $\Delta t = 0.01$, and $T = 1000$.

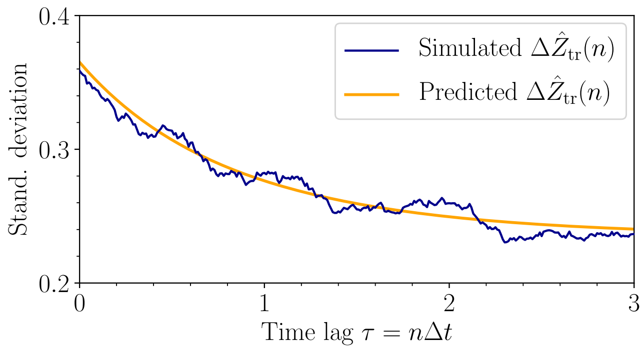


FIG. 7. Standard deviation of the estimator of the mean transient response $\hat{Z}_{\mathrm{tr}}$. The analytical expression obtained from Eq. (25) (orange) is compared to the measured standard deviation of 1000 estimators (blue), which are calculated for distinct ensembles. Each of those ensembles contains $N = 10$ trajectories simulated with parameters $D = 1/11$, $\kappa = 1$, $\varepsilon = 0.2$, $\Delta t = 0.01$, and $T = 1000$.

multiple ensembles and the exact expression for $\langle z_i^{(\mathrm{tr})}(n\Delta t)\rangle$. Figure 6 also demonstrates that the estimator of the mean transient response has stronger fluctuations than the correlation estimator for the given perturbation amplitude. This is due to the fact that the mean transient response is estimated only with an ensemble average, while the correlation estimator includes both an ensemble and a time average.

The statistical fluctuations of $\hat{Z}_{\mathrm{tr}}(n)$ are investigated in more detail by calculating the variance. As before, the covariance of the estimator at different time indices is considered first. The independence of different trajectories allows us to rewrite the covariance as

$$\begin{aligned}\mathrm{Cov}\big(\hat{Z}_{\mathrm{tr}}(n), \hat{Z}_{\mathrm{tr}}(m)\big) &= \frac{1}{N}\mathrm{Cov}\big(z_{i,n}^{(\mathrm{tr})}, z_{i,m}^{(\mathrm{tr})}\big)\\ &= \frac{1}{N}\Big(\big\langle z_{i,n}^{(\mathrm{tr})} z_{i,m}^{(\mathrm{tr})}\big\rangle - \big\langle z_{i,n}^{(\mathrm{tr})}\big\rangle\big\langle z_{i,m}^{(\mathrm{tr})}\big\rangle\Big). \qquad (24)\end{aligned}$$

Inserting the corresponding moments from Appendix A results in a simple expression for the covariance, see Appendix C, and the variance can be read as

$$\mathrm{Var}(\hat{Z}_{\mathrm{tr}}(n)) = \frac{1}{N} e^{2f(n)}(e^{f(0)} - 1), \qquad (25)$$

with $f(j) = e^{-\kappa j \Delta t}\varepsilon^2/\sigma_x^2$. The corresponding prediction of the standard deviation $\Delta\hat{Z}_{\mathrm{tr}} = \sqrt{\mathrm{Var}(\hat{Z}_{\mathrm{tr}}(n))}$ is compared to the measured standard deviation of the estimators of several ensembles. Both curves show good agreement, see Fig. 7.

### D. Uncertainty of the nonlinear fluctuation-dissipation relation

After analyzing the estimators $\hat{Z}_{\mathrm{tr}}$ and $\hat{C}_z$, which are used to approximate the exact statistics in the fluctuation-dissipation relation Eq. (2), it is discussed how their combined uncertainty affects the test of Markovianity. Since deviations from the empirical fluctuation-dissipation relation

$$\hat{Z}_{\mathrm{tr}}(n) = \hat{C}_z(n) \qquad (26)$$

are used as an indication of non-Markovianity, it is relevant to consider the statistics of this deviation in the case of a Markovian system.

A simple measure $\delta$ for a deviation from the empirical nonlinear fluctuation-dissipation relation Eq. (26) at a given time can be defined as $\delta(n) = \hat{Z}_{\mathrm{tr}}(n) - \hat{C}_z(n)$. As both estimators are unbiased, $\langle\delta(n)\rangle = 0$ holds true if the system is Markovian.

The results from Secs. III B and III C can be used to derive an expression for the standard deviation of $\delta$. As all of the derivations assume Markovianity, this standard deviation constitutes a measure for the uncertainty of the deviation $\delta$ in the case of a Markovian system. If the system is Markovian and thus $C_z(\tau) = \langle z_i^{(\mathrm{tr})}(\tau)\rangle$ holds true, a measured deviation from $\delta = 0$ is usually within $[-\Delta\delta, +\Delta\delta]$. In particular, if the measured deviation is not close to this interval, non-Markovianity is likely.

To calculate the standard deviation of $\delta$, the following relation is used:

$$\begin{aligned}\mathrm{Var}(\delta(n)) =& \mathrm{Var}(\hat{Z}_{\mathrm{tr}}(n)) + \mathrm{Var}(\hat{C}_z(n))\\ &- 2\mathrm{Cov}(\hat{Z}_{\mathrm{tr}}(n)\hat{C}_z(n)). \qquad (27)\end{aligned}$$

As stated in the measurement protocol in Sec. I, the estimator $\hat{Z}_{\mathrm{tr}}(n)$ is calculated from the trajectories at $T/2 + n\,\Delta t$ and $\hat{C}_z(n)$ is calculated from trajectories at $t \geqslant 3T/4$. Furthermore, the comparison of both sides of the fluctuation-dissipation relation is only meaningful in a time interval $\tau$ that does not drastically exceed the correlation time $t_c$. At much larger lag times $\tau$, both the correlation between $z_i(\tau_0)$ and $z_i(\tau_0 + \tau)$ (measured in $[3T/4, T]$) as well as the mean value $\tau$ time units after the switch, $\langle z_i^{(\mathrm{tr})}(\tau)\rangle$ (with $\tau = 0$ at $T/2$), will be very close to zero, i.e., the corresponding estimators will be noise dominated. This restriction to sufficiently short intervals for $\tau$ was similarly discussed in Ref. [4].

As long as the quarter of the total measurement window $T$ is much larger than the correlation time $t_c$, i.e., $T/4 \gg t_c$, the relevant parts of the trajectory from the third quarter (used to compute the time-dependent mean value) and the fourth quarter (used to compute the correlation function) are far apart and thus uncorrelated. As a consequence, $\hat{Z}_{\mathrm{tr}}(n)$ and $\hat{C}_z(n)$ are also approximately uncorrelated and $\mathrm{Cov}(\hat{Z}_{\mathrm{tr}}(n)\hat{C}_z(n)) \approx 0$.

Therefore, the variance is simply

$$\mathrm{Var}(\delta(n)) \approx \mathrm{Var}(\hat{Z}_{\mathrm{tr}}(n)) + \mathrm{Var}(\hat{C}_z(n)). \qquad (28)$$

Expressions for both terms on the right-hand side have been derived above. Thus, the standard deviation can be predicted as $\Delta\delta = \sqrt{\mathrm{Var}(\delta)}$. In Fig. 8, the prediction is compared to the measured standard deviation of multiple realizations of $\delta(n) = \hat{Z}_{\mathrm{tr}}(n) - \hat{C}_z(n)$. Each of them is calculated from an independent ensemble of trajectories.

While the above measure $\delta(n)$ characterizes the deviation from the fluctuation-dissipation relation at a single point in time, Ref. [4] proposes to integrate the deviation over a time interval in the following way:

$$\tilde{d} \equiv \frac{\int_0^{T_c} d\tau [\tilde{Z}_{\mathrm{tr}}(\tau) - \tilde{C}_z(\tau)]^2}{\int_0^{T_c} d\tau\, (\tilde{Z}_{\mathrm{tr}}(\tau))^2}, \qquad (29)$$

where $T_c$ is the time until the system has relaxed into the steady state to good approximation. For all the results presented below, this parameter is chosen as $T_c = 10$. This is consistent with the corresponding discussion in [4].

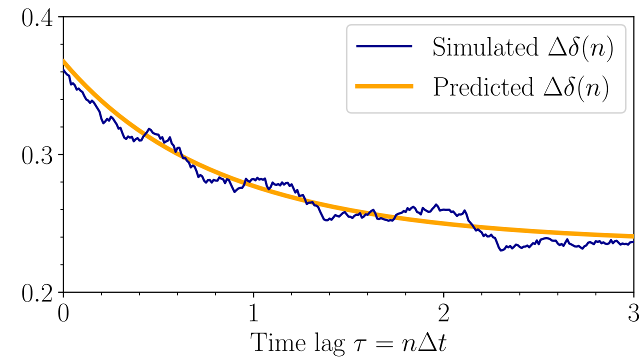


FIG. 8. Standard deviation of the deviation measure $\delta(n)$. The analytical expression obtained from Eq. (28) (orange) is compared to the measured standard deviation of 1000 realizations of $\delta$ (blue), which are calculated for distinct ensembles. Each of these ensembles contains $N = 10$ trajectories simulated with $D = 1/11$, $\kappa = 1$, $\varepsilon = 0.2$, $\Delta t = 0.01$, and $T = 1000$. As before, the correlation estimator is obtained from trajectories with $N_T = 25001$ steps.

Calculating the moments of $\tilde{d}$ is difficult due to the random variable $\hat{Z}_{\mathrm{tr}}$ in the denominator. A drastic simplification is achieved by replacing the estimator in the denominator by its exact counterpart. The denominator was introduced to normalize the deviation [4], which is necessary for comparability between different perturbation amplitudes. This purpose of the denominator is not affected too much by the replacement.

After discretizing the integral, the new deviation measure $d$ reads

$$d \equiv \frac{\sum_{n=0}^{n_c}[\hat{Z}_{\mathrm{tr}}(n) - \hat{C}_z(n)]^2}{\sum_{n=0}^{n_c}\left\langle z_{i,n}^{(\mathrm{tr})}\right\rangle^2}, \tag{30}$$

with $n_c = T_c/\Delta t - 1 = 999$. A shorthand notation for the denominator is introduced:

$$f \equiv \sum_{n=0}^{n_c}\left\langle z_{i,n}^{(\mathrm{tr})}\right\rangle^2. \tag{31}$$

Since the new deviation measure $d$ is of second order in the estimators, its mean value does not vanish:

$$\langle d\rangle = \frac{1}{f}\sum_{n=0}^{n_c}\left[\left\langle \hat{Z}_{\mathrm{tr}}^2(n)\right\rangle + \left\langle \hat{C}_z^2(n)\right\rangle - 2\langle \hat{Z}_{\mathrm{tr}}(n)\hat{C}_z(n)\rangle\right]. \tag{32}$$

For $n_c\Delta t \ll T/4$, both estimators are separated by a sufficiently long time and thus approximately uncorrelated, i.e., $\langle \hat{Z}_{\mathrm{tr}}(n)\hat{C}_z(n)\rangle = \langle \hat{Z}_{\mathrm{tr}}(n)\rangle\langle \hat{C}_z(n)\rangle$ [cf. discussion following Eq. (27)]. We verified by an analytical calculation of the mixed moment that this approximation holds true for all $\varepsilon \in (0, 1]$ for the given simulation parameters. Due to Markovianity, the fluctuation-dissipation relation can be applied to rewrite

$$2\langle \hat{Z}_{\mathrm{tr}}(n)\rangle\langle \hat{C}_z(n)\rangle = \langle \hat{C}_z(n)\rangle^2 + \langle \hat{Z}_{\mathrm{tr}}(n)\rangle^2 \tag{33}$$

and it thus follows

$$\langle d\rangle \approx \frac{1}{f}\sum_{n=0}^{n_c}[\mathrm{Var}(\hat{Z}_{\mathrm{tr}}(n)) + \mathrm{Var}(\hat{C}_z(n))]. \tag{34}$$

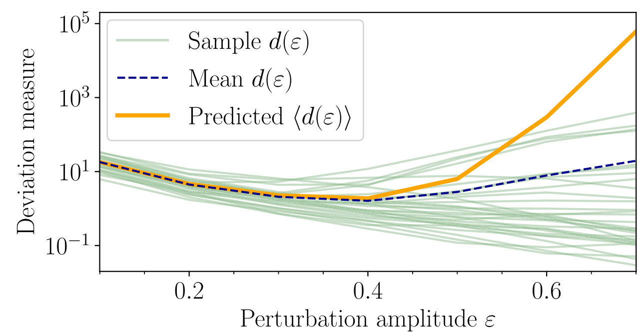


FIG. 9. Deviation measure $d$ at different perturbation amplitudes $\varepsilon$. The prediction Eq. (34) (orange) is compared to 31 realizations (green) and the mean over 100 realizations of $d$ (blue), which are calculated for distinct ensembles. Each of these ensembles contains $N = 10$ trajectories simulated with $D = 1/11$, $\kappa = 1$, $\Delta t = 0.01$, and $T = 1000$. The correlation estimator is obtained from trajectories with $N_T = 25001$ steps.

Both contributions on the right-hand side, $S_Z \equiv \frac{1}{f}\sum_{n=0}^{n_c}\mathrm{Var}(\hat{Z}_{\mathrm{tr}}(n))$ and $S_C \equiv \frac{1}{f}\sum_{n=0}^{n_c}\mathrm{Var}(\hat{C}_z(n))$, can be calculated with the expressions derived above. The prediction $\langle d\rangle$ is compared to multiple realizations of $d$ Eq. (30), each calculated from a new ensemble, and to the mean of these realizations. This comparison is shown for different perturbation amplitudes $\varepsilon$ in Fig. 9. The predicted curve as well as the mean simulation result both have a minimum close to the standard deviation $\varepsilon_{\min} \approx \sigma_x \approx 0.3$. This is similar to the results in Ref. [4], where the conjugated variable $z(x)$ was estimated from Eq. (3) with measured probability densities. In Ref. [4], the increasing deviation for $\varepsilon \gg \sigma_x$ was attributed to the insufficient statistics in the tails of the probability densities $P_0(x)$ and $P_\varepsilon(x)$ which contribute to a large random error in $z(x)$ estimates. This explanation does not apply to our result in Fig. 9 because the conjugated variable $z(x)$ is now exact.

Instead, the large deviation for $\varepsilon \gg \sigma_x$ is caused by the contribution of the correlation function, i.e., $S_C \gg S_Z$ as depicted in Fig. 10. The uncertainties in the correlation function are connected to a strongly intermittent behavior of $z(x(t))$. For large $\varepsilon$, a large part of the $x$ axis is compressed into a

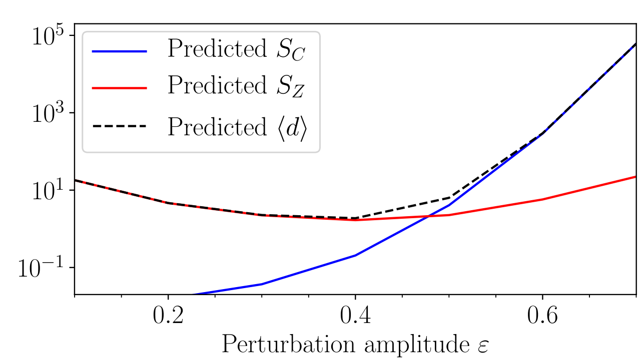


FIG. 10. Predicted contributions to $\langle d\rangle = S_Z + S_C$ at different perturbation amplitudes. The curves are calculated for parameters $D = 1/11$, $\kappa = 1$, $\Delta t = 0.01$, $N_T = 25001$, and $N = 10$ trajectories per ensemble.

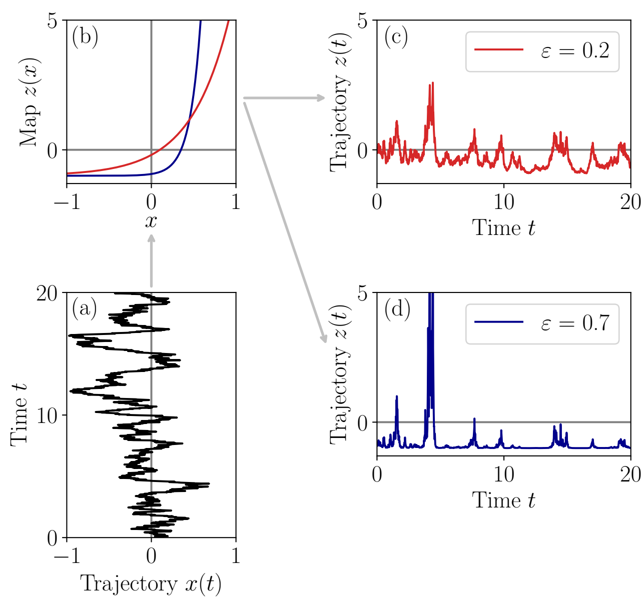


FIG. 11. Transformation behavior of $z(x)$ at different perturbation amplitudes. A trajectory $x(t)$ simulated with parameters $D = 1/11$, $\kappa = 1$, and $\Delta t = 0.01$ in the stationary unperturbed state is shown in (a) and inserted into the map $z(x)$ in (b) at $\varepsilon = 0.2$ and $\varepsilon = 0.7$, respectively. The resulting trajectories $z(t)$ are depicted in (c) and (d).

small interval on the $z$ axis while strongly positive values of $x$ result in extremely high but rare peaks in $z$ (cf. Fig. 11). Both the strong compression and the rare peaks obstruct a reliable estimation of the correlation function $C_z(\tau)$.

The significant deviation between predicted average and observed mean for $\varepsilon \geqslant 0.5$ is discussed in Sec. III E.

As for the simpler deviation measure $\delta$, the standard deviation of $d$ is used to characterize its statistical uncertainty. If a measured value of $d$ is far outside of this interval $[\langle d\rangle - \Delta d, \langle d\rangle + \Delta d]$, the system is likely not Markovian.

Before calculating the variance of $d$ it is useful to rewrite the quantity in the following way:

$$\begin{aligned} d =& \frac{1}{f}\sum_{n=0}^{n_c}(\hat{C}_z(n) - \langle\hat{C}_z(n)\rangle)^2 \\ &+ \frac{1}{f}\sum_{n=0}^{n_c}(\hat{Z}_{\mathrm{tr}}(n) - \langle\hat{Z}_{\mathrm{tr}}(n)\rangle)^2 \\ &- \frac{2}{f}\sum_{n=0}^{n_c}(\hat{C}_z(n) - \langle\hat{C}_z(n)\rangle)(\hat{Z}_{\mathrm{tr}}(n) - \langle\hat{Z}_{\mathrm{tr}}(n)\rangle). \end{aligned} \tag{35}$$

For details on this step, see Appendix D. In this expression, all random variables are centered, which is the prerequisite for the following calculation. The variance is obtained as

$$\mathrm{Var}(d) = \langle d^2\rangle - \langle d\rangle^2. \tag{36}$$

Inserting Eq. (35) yields a sum of centered moments up to fourth order. As before, all mixed moments factorize into moments in $\hat{C}_z$ and moments in $\hat{Z}_{\mathrm{tr}}$. The expression is given in Appendix D.

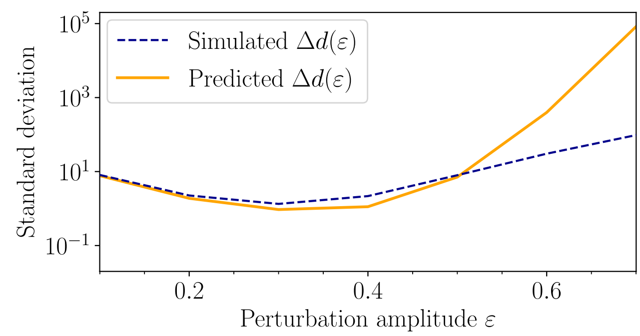


FIG. 12. Standard deviation of the deviation measure $d$ at different perturbation amplitudes $\varepsilon$. The prediction obtained from Eq. (37) (orange) is compared to the empirical standard deviation of 100 realizations of $d$ (blue), which are calculated for distinct ensembles. Each of these ensembles contains $N = 10$ trajectories simulated with $D = 1/11$, $\kappa = 1$, $\Delta t = 0.01$, and $T = 1000$. The correlation estimator is obtained from trajectories with $N_T = 25001$ steps.

All these moments could be calculated exactly by following the basic scheme of Secs. III B and III C: The moments of estimators are rewritten as moments of $z_{i,j}$, which in turn can be calculated using the approach presented in Appendix A. The resulting expressions are expected to be lengthy and not very practical. A drastic simplification can be obtained if the estimators themselves are approximated to follow a normal distribution. As a consequence, all higher order centered moments in the estimators can be reduced to second moments, see, e.g., [3] (Eq. 2.8.4 therein). The approximation of a normal distribution for the estimators is based on the central limit theorem. Both $\hat{C}_z$ and $\hat{Z}_{\mathrm{tr}}$ include a sum over independent realizations. For sufficiently large numbers of trajectories $N$, the central limit theorem predicts the normal distribution. Within this approximation, the following expression for the variance of the deviation measure $d$ is obtained, see Appendix D:

$$\begin{aligned} \mathrm{Var}(d) =& \frac{4}{f^2}\sum_{i=1}^{n_c}\sum_{j=0}^{i-1}[\mathrm{Covar}(\hat{C}_z(i), \hat{C}_z(j)) \\ &+ \mathrm{Covar}(\hat{Z}_{\mathrm{tr}}(i), \hat{Z}_{\mathrm{tr}}(j))]^2 \\ &+ \frac{2}{f^2}\sum_{i=0}^{n_c}[\mathrm{Var}(\hat{C}(i)) + \mathrm{Var}(\hat{Z}_{\mathrm{tr}}(i))]^2. \end{aligned} \tag{37}$$

This calculation of $\mathrm{Var}(d)$ follows the basic steps that are used to derive expressions for error propagation in experimental physics: The variance of the outcome variable $d$ is expressed in terms of the covariances of the input variables $\hat{Z}_{\mathrm{tr}}(m)$ and $\hat{C}(n)$. For a linear approximation of the outcome variable as a function of the input variables, a detailed calculation can be found in [21] (Sec. 3.7.1 therein). The result of a second-order approximation expanded around a critical point is stated in [21] [Eq. (4.138) is assumed to be a special case of Eq. (4.140) therein]. It is consistent with Eq. (37) since $d$ is a multivariate polynomial of degree two and the exact equation Eq. (35) coincides with the second-order Taylor expansion.

The corresponding prediction for the standard deviation $\Delta d = \sqrt{\mathrm{Var}(d)}$ is compared to the measured standard deviation of multiple realizations of $d$ in Fig. 12. The simulated

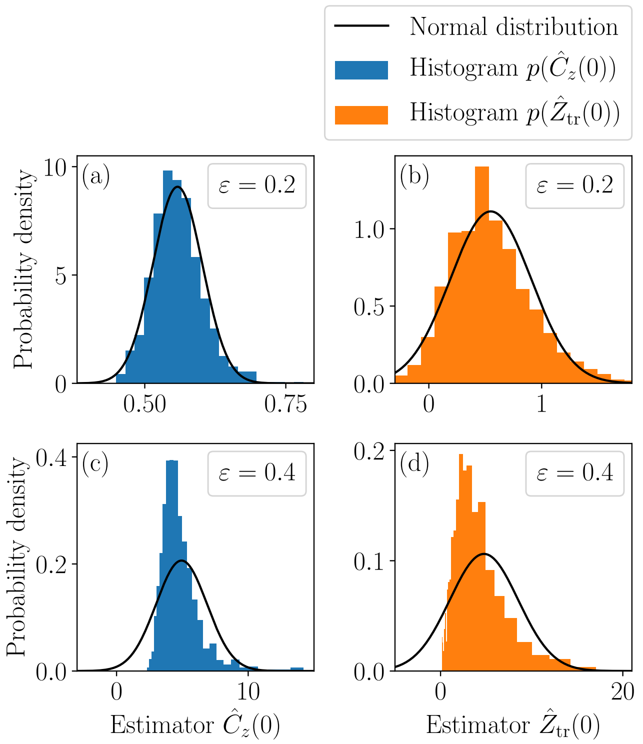


FIG. 13. Histograms of the correlation estimator $\hat{C}_z(0)$ (left) and the mean transient estimator $\hat{Z}_{tr}(0)$ (right) for perturbation amplitudes $\varepsilon = 0.2$ (top) and $\varepsilon = 0.4$ (bottom). Each histogram contains 1000 estimators which are calculated for distinct ensembles. Each of these ensembles contains $N = 10$ trajectories simulated with $D = 1/11$, $\kappa = 1$, $\Delta t = 0.01$, and $N_T = 25001$ steps which correspond to $T = 1000$. The standard deviation and mean of each histogram is used to determine the respective normal distribution as comparison.

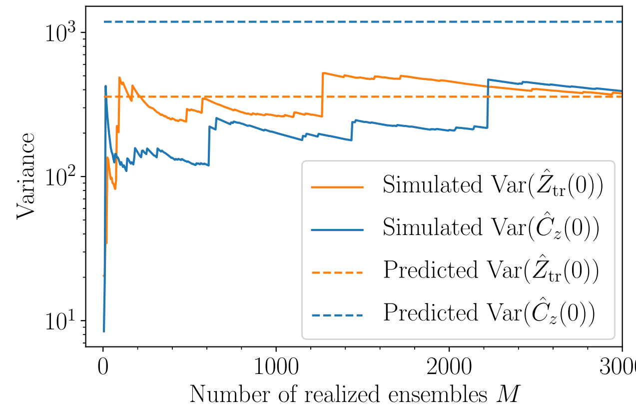


FIG. 14. Observed variance of $M$ estimators of the correlation function and the mean transient response $\hat{C}_z(0)$ and $\hat{Z}_{tr}(0)$ which are calculated for distinct ensembles. Each of these ensembles contains $N = 10$ trajectories simulated with $D = 1/11$, $\kappa = 1$, $\Delta t = 0.01$, $N_T = 25001$ corresponding to $T = 1000$ and a perturbation amplitude $\varepsilon = 0.5$. The predicted values are obtained from Eq. (C4) and Eq. (25).

curve deviates from the predicted curve at $\varepsilon > 0.5$ in a similar way as for the respective $\langle d \rangle$ curves in Fig. 9. This deviation is also addressed in the discussion in Sec. III E. Apart from this observation, it seems that the approximation of normally distributed estimator results is a good prediction of $\Delta d$ for perturbation strengths $\varepsilon \leqslant 0.3$, even for a relatively small number of trajectories $N = 10$. The deviation at intermediate values of $0.3 < \varepsilon \leqslant 0.5$, which has the opposite sign of the deviation for $\varepsilon > 0.5$, might be due to the breakdown of this approximation. This hypothesis is supported by Fig. 13, which shows that the distribution of the exemplary estimators $\hat{C}_z(0)$ and $\hat{Z}_{tr}(0)$ is close to a normal distribution at $\varepsilon = 0.2$ but far off at $\varepsilon = 0.4$.

### E. Effect of heavy tails on the simulation results

The simulation results for the mean and standard deviations of $d$ show a large deviation from the predicted curves in Figs. 9 and 12 at large perturbation amplitudes $\varepsilon \geqslant 0.5$. For the simpler case of $\langle d \rangle$, Eq. (34) shows that the average of the deviation measure depends on the variances of the statistical estimators. Hence, a deviation of the empirical variance of a finite ensemble of estimators from their true variance is connected to a deviation of the corresponding $\langle d \rangle$.

For the case of the time index $n = 0$, the convergence behavior of the empirical variance of $M$ estimators $\hat{C}_z(n)$ and $\hat{Z}_{tr}(n)$ toward their respective predicted true variance is shown in Fig. 14. This is done at a relatively large perturbation strength of $\varepsilon = 0.5$ at which the original deviation in Fig. 9 is already apparent.

At large values of $M \sim 10^3$, the empirical variance of $\hat{Z}_{tr}(0)$ is close to the exact value while the corresponding value of $\hat{C}_z(0)$ is far off from its true value. This suggests that the deviation observed in Fig. 9 might be due to the fact that the empirical variance of 100 correlation estimators has not converged to the exact value of the variance.

This hypothesis is supported by Fig. 13, which indicates that larger $\varepsilon$ values might be connected to an increased right tail of the distribution. As a consequence, extremely large values of $\hat{C}_z$ have a higher contribution to the value of the variance. If those rare events are not realized in a given finite ensemble, the variance is underestimated.

To test this explanation, the distribution of $\hat{C}_z(0)$ at $\varepsilon = 0.5$ is measured in a histogram, see Fig. 15, and a model probability distribution $p(\hat{C}_z(0))$ with the following properties is determined:

(1) The model distribution $p(\hat{C}_z(0))$ is consistent with the predicted average and variance of $\hat{C}_z(0)$, which have been derived in Sec. III B. In addition to the correct normalization, this leads to conditions for the first and second moments of the distribution.

(2) The model distribution roughly resembles the measured histogram of $\hat{C}_z(0)$.

(3) The model distribution has a heavy right tail. For simplicity $p(\hat{C}_z(0)) \sim \hat{C}_z(0)^{-\alpha}$ is chosen.

It was found that all of these conditions can be met to good approximation if the left part of the histogram, i.e., $\hat{C}_z(0) < \hat{C}_{\text{threshold}}$, is directly used as a distribution and the right part, i.e., $\hat{C}_z(0) \geqslant \hat{C}_{\text{threshold}}$, is replaced with the tail $\sim\hat{C}_z(0)^{-\alpha}$. The details of this analysis are presented in Appendix E. The histogram as well as the model tail are depicted in Fig. 15.

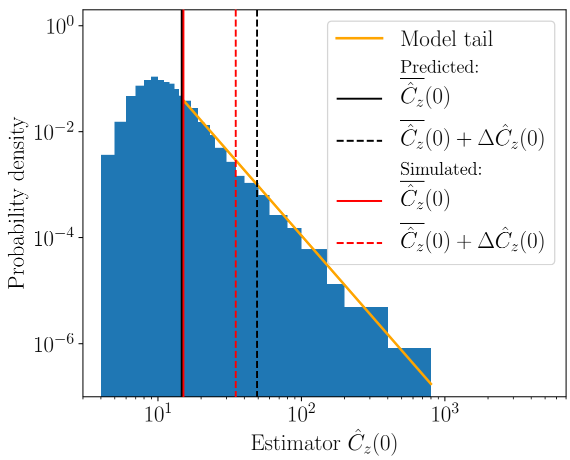


FIG. 15. Histogram of the correlation estimator $\hat{C}_z(0)$. It contains $M = 3000$ estimators, which are calculated for distinct ensembles. Each of these ensembles contains $N = 10$ trajectories simulated with $D = 1/11$, $\kappa = 1$, $\Delta t = 0.01$, and $N_T = 25\,001$, corresponding to $T = 1000$ and a perturbation amplitude $\varepsilon = 0.5$. The mean and the sum of mean and standard deviations, which are observed for the measured histogram of simulation results (red), are compared to the corresponding predictions obtained from Eqs. (12) and (C4) (black). The distribution tail, which is modeled in accordance with the predictions, is indicated (orange).

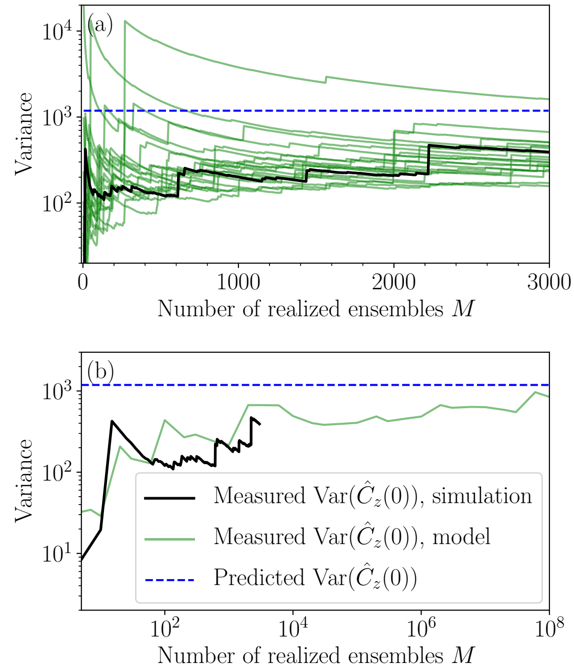


FIG. 16. Convergence behavior of the variance of the correlation estimator. The measured variance of an ensemble of $M$ estimators $\hat{C}_z(0)$ obtained from simulation (black) (each for distinct ensembles of $N = 10$ trajectories and parameters $D = 1/11$, $\kappa = 1$, $\Delta t = 0.01$, $N_T = 25\,001$, $T = 1000$, $\varepsilon = 0.5$) is compared to the corresponding value if $\hat{C}_z(0)$ is not calculated from simulation results but directly drawn from the model distribution [green, 20 realizations are depicted in (a)]. The predicted variance of $\hat{C}_z(0)$ distribution obtained from Eq. (C4) is depicted in blue.

The fact that a distribution could be found which has approximately the correct mean and standard deviation and which is also very close to the observed histogram strongly supports the hypothesis that the difference between empirical and exact variance in Fig. 14 and thus, ultimately, also the deviation in Fig. 9, is simply due to a slow convergence behavior and not due to an error in the prediction. As an additional check, it is investigated whether the sample variance of random numbers drawn from the model distribution has a similar convergence behavior to the predicted value as the empirical variance of $\hat{C}_z(0)$ obtained from simulations. Figure 16 shows that this is the case. Furthermore, it indicates that the sample variance of the model distribution gets close to the predicted variance only at very large ensembles of $\sim 10^8$ realizations.

The deviation observed in Fig. 12 for large $\varepsilon$ values might be caused by the same effect since the analytic expression for the variance Eq. (37) also includes the variance of the correlation estimator.

The main limitation of the explanation is the fact that the tail $\hat{C}_z(0)^{-\alpha}$, which was used for the model distribution, is too heavy to describe the actual distribution. While this power-law tail would result in diverging higher moments $\langle \hat{C}_z^n(0) \rangle$, see, e.g., [22] (Sec. 3 therein), the calculation scheme in Appendix C demonstrates that any moment in $\hat{C}_z(0)$ can be written as a finite sum of moments of $z(x(t))$. All these moments of the conjugated variable are finite, as obvious from Appendix A. Hence, also all moments in the correlation estimator must be finite. This apparent contradiction can be resolved by assuming that the description of the distribution with a power-law tail is a good approximation in a finite interval of $\hat{C}_z(0)$. If the parameter $\alpha$ in $\hat{C}_z(0)^{-\alpha}$ is itself a slowly increasing function of $\hat{C}_z(0)$, the tail is slimmer than a power-law tail and the distribution can have finite higher moments. As long as $\alpha = \alpha(\hat{C}_z(0))$ increases sufficiently slowly, it can be approximated by a constant value for the relevant section of the $\hat{C}_z(0)$ axis in Fig. 15. In this case, the power-law description is a valid approximation for the histogram.

This argument is illustrated by the example of a log-normal distribution. Its probability density is given by [23] (p. 28 therein)

$$p(x) = \frac{1}{\sqrt{2\pi}\sigma x} \exp\left[-\frac{1}{2}\left(\frac{\ln(x) - \mu}{\sigma}\right)^2\right]. \tag{38}$$

If the tail of this distribution is modeled as $\sim x^{-\alpha(x)}$, the exponent is determined by calculating the logarithmic derivative of the distribution function. With $y \equiv \ln(x)$, this can be written as

$$\begin{aligned} -\alpha(x) &= \frac{d\ln(p(x))}{d\ln(x)} \\ &= \frac{d}{dy}\ln\left\{\frac{1}{\sqrt{2\pi}\sigma e^y}\exp\left[-\frac{1}{2}\left(\frac{y-\mu}{\sigma}\right)^2\right]\right\} \\ &= \frac{d}{dy}\ln\left\{\exp\left[-\frac{1}{2}\left(\frac{y-\mu}{\sigma}\right)^2\right]\right\} + \frac{d}{dy}\ln\left\{\frac{1}{\sqrt{2\pi}\sigma e^y}\right\} \end{aligned}$$

$$= -\frac{1}{2}\frac{d}{dy}\left(\frac{y-\mu}{\sigma}\right)^2 - 1$$
$$= \frac{\mu - \ln(x)}{\sigma^2} - 1. \tag{39}$$

This shows that $\alpha(x)$ increases logarithmically and may be approximated as a constant for a section of the tail. This similarity between a log-normal distribution and a power-law tail is also discussed in [22] (Sec. 3.3.2 therein).

## IV. DISCUSSION

The present work investigates the statistical reliability of a test for Markovianity, which was proposed in Ref. [4]. The test relies on a nonlinear fluctuation-dissipation relation, which holds under the assumption of Markovianity. This relation compares the correlation function to the mean transient response to a steplike perturbation in terms of a conjugated variable $z(t)$. If a violation of this relation occurs for the true statistics of a given system, it can be concluded that it is non-Markovian. Since only finite-size estimators of the statistics are experimentally accessible, small deviations from the NL-FDR will be observed even for Markovian systems. To make a reliable statement on non-Markovianity of the system at hand, the magnitude of these finite-size deviations must be known for the Markovian case: If an observed deviation from the NL-FDR is within the bounds of statistical uncertainty of the estimators of the Markovian system, no conclusion on its non-Markovianity is possible. If the deviations are much larger, they can no longer be explained solely by measurement effects and the non-Markovianity of the system appears plausible.

Here, we derived expressions for the variance of the empirical correlation and the empirical mean transient, as well as their combined uncertainty at a single point in time. For an integrated deviation measure, which characterizes the violation of the NL-FDR over a time interval, an exact expression is introduced for the mean value and an approximation is presented for the standard deviation.

We provide a theoretical calculation of the minimum in the integrated deviation measure at intermediate perturbation amplitudes, which was already observed in simulation data [4]. The persistence of the minimum is remarkable since in our discussion, one of the sources of uncertainty thought to be responsible for the increase of the deviation at larger perturbation amplitudes is suppressed; namely, the poorly measured tails of the histograms entering the calculation of $\hat{z}(x)$ [4]. Our results suggest that the effect is instead caused by the increasingly intermittent behavior of the nonlinear transformation $x(t) \to z(t)$ at large $\varepsilon$ values. Preliminary simulations indicate that if we also take into account the contribution of the error-prone estimate $\hat{z}(x)$ of the conjugated variable $z(x)$, this does not have much of an effect at small to intermediate perturbation amplitudes $\varepsilon$, while for large amplitudes it is more complicated: The additional complication is connected to empty histogram bins, and the results depend strongly on how this problem is handled.

It is also demonstrated that strong perturbations lead to large differences between predicted and observed statistics. As discussed in Sec. III E, this is suspected to be due to heavy-tailed distributions for some of the estimators, which cause a slow convergence behavior of the sample statistics towards their true values.

Similar numerical problems for large perturbation amplitudes are expected to arise in systems with a nonlinear but bounding potential $U_0(x)$ that are perturbed by a constant force $\varepsilon$, for which we find from the Boltzmann distributions $P_0(x)$ and $P_\varepsilon(x)$:

$$z(x) = C\exp\left[\varepsilon x/D\right] - 1, \tag{40}$$

i.e., again an exponentially growing function that strongly amplifies positive deviations in $x$. For practical applications, it might be of importance to look for a specific kind of perturbation with which we can avoid or mitigate the above discussed complications. One example would be a multiplicative change of a parabolic potential by switching the curvature from a small value to a large value at $t = T/2$ [24,25], for which we obtain the conjugated variable of the form

$$z(x) = \sqrt{1+\frac{\varepsilon}{k}}\exp\left[-\frac{\varepsilon x^2}{2D}\right] - 1, \tag{41}$$

a Gaussian that might be suitable to avoid the intermittent behavior. The detailed investigation of this question is beyond the scope of our study but constitutes an interesting problem for future research.

The position and depth of the minimum in the deviation measure, both of which are of great interest when planning an experiment to test Markovianity, can be found numerically from the expressions Eqs. (34) and (37). As a rule of thumb, the optimal perturbation is on the onset of nonlinear response, where it evokes a deviation in the time-dependent mean that is of the order of one standard deviation of the spontaneous (unperturbed) fluctuations of the system. Significantly larger perturbation amplitudes lead to a reduced overlap between the two probability densities $P_0(x)$ and $P_\varepsilon(x)$ and, consequently, to a strongly nonlinear mapping $z(x)$ that renders the determination of the statistics appearing in the NL-FDR difficult. This concerns in particular the determination of the correlation function.

Furthermore, the analytical results also allow for the investigation of other optimization strategies. As already pointed out in [4], the time intervals in the measurement protocol might be changed. Keeping the total measurement time $NT$ constant and increasing the number of realizations $N$ while decreasing the time per realization $T$ affects the uncertainty of both estimators in the NL-FDR in different ways. It remains an interesting task to determine the optimal ratio of both variables.

## ACKNOWLEDGMENT

This research was funded by the Deutsche Forschungsgemeinschaft (DFG, German Research Foundation), Grant No. LI 1046/15-1.

## DATA AVAILABILITY

The data that support the findings of this article are openly available [26].

## APPENDIX A: MOMENTS OF $x$ AND $z$

The statistics of the estimators $\hat{C}_x$, $\hat{C}_z$, and $\hat{Z}_{\mathrm{tr}}$ are expressed in terms of moments of the original variable $x$ and the conjugated variable $z$. These moments are of the type $\langle x_{i,j}x_{k,l}\ldots\rangle$, $\langle z_{i,j}z_{k,l}\ldots\rangle$, and $\langle z_{i,j}^{(\mathrm{tr})}z_{k,l}^{(\mathrm{tr})}\ldots\rangle$. For the calculation of these moments, the multivariate distributions of the random variables $\{x_{i,j}^{(\mathrm{tr})}\}$ and $\{x_{i,j}\}$, i.e., the trajectories of the Ornstein-Uhlenbeck process during $t\in[T/2,3T/4]$ and $t\in[3T/4,T]$ must be known. Due to the independence of multiple realizations and the factorization of the corresponding moments, it suffices to consider the distribution of a single realization, and thus the realization index is omitted for simplicity.

An unperturbed Ornstein-Uhlenbeck process, $X_t$ initialized at a given point $X_0$ at $t=0$ is a Gaussian process which means that any subset of its values $\{X_{t_1},X_{t_2},\ldots\}$ follows a multivariate normal distribution [23] (Sec. 8.5 therein). Following the measurement protocol, the trajectories are not initialized at a given point at $T/2$ or $3T/4$. Nevertheless, the sets of random variables $\{x_j^{(\mathrm{tr})}\}$ and $\{x_j\}$ each follow a multivariate normal distribution. This can be seen if the multivariate distribution is constructed from the transition probabilities of the Ornstein-Uhlenbeck process [1] [Eq. (5.28) therein]:

$$p(x,t|x_0,0)=\sqrt{\frac{1}{2\pi\sigma_x^2(1-e^{-2\kappa t})}}\exp\left[-\frac{\left(x-x_0e^{-\kappa t}\right)^2}{2\sigma_x^2(1-e^{-2\kappa t})}\right]\tag{A1}$$

and an initial probability density [4]

$$p_0(x)=\frac{1}{\sqrt{2\pi\sigma_x^2}}\exp\left[-\frac{(x-\mu)^2}{2\sigma_x^2}\right],\tag{A2}$$

with $\mu=0$ in the case of the steady-state trajectory $\{x_i\}$. The expressions also hold true for the transient trajectory $\{x_i^{(\mathrm{tr})}\}$. In this case, the initial distribution is centered at $\mu=\varepsilon$. The multivariate distribution reads

$$\begin{aligned}&p(x_{N_T-1},t_{N_T-1};\ldots;x_0)\\&=p(x_0)\prod_{j=1}^{N_T-1}p(x_j,t_j\,|\,x_{j-1},t_{j-1})\\&=c\exp\left[-\frac{\mu^2-2\mu x_0+x_0^2}{2\sigma_x^2}-\sum_{j=1}^{N_T-1}\frac{\left(x_j-x_{j-1}e^{-\kappa\Delta t}\right)^2}{2\sigma_x^2(1-e^{-2\kappa\Delta t})}\right],\end{aligned}\tag{A3}$$

with normalization factor $c$. This can be identified as a multivariate normal distribution in the notation given in [2] (p. 24 therein),

$$p(x_{N_T-1},\ldots,x_0)=\tilde{c}\exp\left[-\frac{1}{2}\sum_{i,j=0}^{N_T-1}A_{ij}x_ix_j-\sum_{i=0}^{N_T-1}B_ix_i\right],\tag{A4}$$

with a positive definite matrix $A$, being the inverse of the covariance matrix. To fully characterize these normal distributions for $\{x_i^{(\mathrm{tr})}\}$ and $\{x_i\}$, respectively, it is sufficient to know the covariances and the means.

The covariance matrix of this multivariate normal distribution is solely determined by the correlation function of the Ornstein-Uhlenbeck process Eq. (11). It is independent of whether the steady-state trajectory $\{x_i\}$ or the transient trajectory $\{x_i^{(\mathrm{tr})}\}$ is considered. For an initialization of the Ornstein-Uhlenbeck process at a random variable $x_0$ with a variance $\mathrm{Var}(x_0)$, the covariance at time indices $i\geqslant j\geqslant 0$ is given by [27] [Eq. (5) therein with modifications]

$$\begin{aligned}\mathrm{Cov}(x_i,x_j)=&\frac{D}{\kappa}e^{-\kappa i\Delta t}\left(e^{\kappa j\Delta t}-e^{-\kappa j\Delta t}\right)\\&+e^{-\kappa(i+j)\Delta t}\mathrm{Var}(x_0).\end{aligned}\tag{A5}$$

In this expression, $x_i$ can be replaced by $x_i^{(\mathrm{tr})}$. The initial values $x_0$ and $x_0^{(\mathrm{tr})}$ are drawn from the distributions at $t=T/2$ or $t=3T/4$, respectively, which both have a variance of $\sigma_x^2=D/\kappa$ as discussed in Ref. [4]. Therefore, the above expression can be rewritten as

$$\begin{aligned}\mathrm{Cov}\left(x_i^{(\mathrm{tr})},x_j^{(\mathrm{tr})}\right)&=\mathrm{Cov}(x_i,x_j)\\&=\frac{D}{\kappa}e^{-\kappa(i-j)\Delta t}.\end{aligned}\tag{A6}$$

By generalizing this expression to arbitrary orderings of $i$ and $j$, the absolute value emerges; for a different derivation, the second moment in Ref. [28] can be used. Thus, both for the transient as well as for the steady-state multivariate normal distribution, the covariance is given by

$$\begin{aligned}\mathrm{Cov}\left(x_i^{(\mathrm{tr})},x_j^{(\mathrm{tr})}\right)=\mathrm{Cov}(x_i,x_j)&=C_x((i-j)\Delta t)\\&=\frac{D}{\kappa}e^{-\kappa|i-j|\Delta t}.\end{aligned}\tag{A7}$$

The mean is simply $\langle x_i\rangle=0$ in the steady state and $\langle x_i^{(\mathrm{tr})}\rangle=\varepsilon e^{-\kappa\, i\Delta t}$ in the transient state, as discussed in Ref. [4].

As a consequence of the Gaussianity of $x$, all (mixed) moments of $x$ in the steady state are known, see, e.g., [3] [Eq. (2.8.4) therein]; the relation is also known as Wick's or Isserlis's theorem. In particular, the odd moments vanish and

$$\langle x_{i,k}x_{i,l}\rangle=C_x[(k-j)\Delta t]\tag{A8}$$

and

$$\begin{aligned}&\langle x_{i,k}x_{i,k+m}x_{i,l}x_{i,l+m}\rangle\\&\quad=\{C_x[m\Delta t]\}^2+\{C_x[(l-k)\Delta t]\}^2\\&\qquad+C_x[(m+l-k)\Delta t]C_x[(m+k-l)\Delta t];\end{aligned}\tag{A9}$$

see also [28]. In these expressions, the realization index was reintroduced. These moments are used in the calculation of $\mathrm{Var}(\hat{C}_x(n))$. For the statistics of $\hat{C}_z(n)$ and $\hat{Z}_{\mathrm{tr}}(n)$ the moments of $z$ are needed, both in the transient state $z_{i,k}^{(\mathrm{tr})}=z(x_{i,k}^{(\mathrm{tr})})$ and the steady state $z_{i,k}=z(x_{i,k})$ of the process. These moments can be calculated by exploiting the structure of the nonlinear transformation Eq. (7), i.e., $z(x)=a\,e^{bx}+c$. For an exponential transformation $ae^{bx}$ of a Gaussian random variable, i.e., a log-normal random variable, the moments are known. As explained in Ref. [29] (p. 233 therein), the comparison of the moment $\langle ae^{bx}\rangle$ to the characteristic function $\tilde{\Theta}(s)\equiv\langle e^{\mathrm{i}xs}\rangle$ shows

$$\langle ae^{bx}\rangle=a\tilde{\Theta}(-\mathrm{i}b),\tag{A10}$$

which can be easily evaluated since the characteristic function of the normal distribution is known. As shown above, both $\{x_j^{(\mathrm{tr})}\}$ and $\{x_j\}$ follow a multivariate normal distribution for which the corresponding covariance and mean are known. Therefore, the characteristic functions of these distributions are also known, and the above method can be generalized to higher moments; see Ref. [30]. After modifications, this yields

$$\begin{aligned}&\left\langle \exp\left(bx_{m_1}^{(\mathrm{tr})}\right)\exp\left(bx_{m_2}^{(\mathrm{tr})}\right)\ldots\exp\left(bx_{m_n}^{(\mathrm{tr})}\right)\right\rangle\\&\quad=\exp\left(b\varepsilon\sum_{k\in\{m_i\}}e^{-\kappa k\Delta t}+\frac{1}{2}b^2\sum_{k,l\in\{m_i\}}C_x((k-l)\Delta t)\right)\end{aligned}\tag{A11}$$

and

$$\begin{aligned}&\langle\exp(bx_{m_1})\exp(bx_{m_2})\ldots\exp(bx_{m_n})\rangle\\&\quad=\exp\left(\frac{1}{2}b^2\sum_{k,l\in\{m_i\}}C_x((k-l)\Delta t)\right),\end{aligned}\tag{A12}$$

with general time indices $m_i\in\{0,\ldots,N_T-1\}$. By going from a purely exponential transformation to $z(x)$, the following moments are derived. Some of these expressions are already included in Ref. [4]; the complete list of needed expressions reads as follows:

$$\left\langle z_{i,k}^{(\mathrm{tr})}\right\rangle=e^{f(k)}-1,\tag{A13}$$

$$\langle z_{i,k}\rangle=0,\tag{A14}$$

$$\left\langle z_{i,k}^{(\mathrm{tr})}z_{i,l}^{(\mathrm{tr})}\right\rangle=e^{f(k)+f(l)+f(|l-k|)}-e^{f(k)}-e^{f(l)}+1,\tag{A15}$$

$$\langle z_{i,k}z_{i,l}\rangle=e^{f(|k-l|)}-1,\tag{A16}$$

and

$$\begin{aligned}&\langle z_{i,l}z_{i,l+n}z_{i,k}z_{i,k+m}\rangle\\&\quad=-3+e^{f(|m|)}+e^{f(|n|)}+e^{f(|l-k|)}\\&\qquad+e^{f(|l-k+n|)}+e^{f(|k-l+m|)}+e^{f(|l-k+n-m|)}\\&\qquad-e^{f(|m|)+f(|l-k|)+f(|k-l+m|)}\\&\qquad-e^{f(|n|)+f(|l-k|)+f(|l-k+n|)}\\&\qquad-e^{f(|m|)+f(|l-k+n|)+f(|l-k+n-m|)}\\&\qquad-e^{f(|n|)+f(|k-l+m|)+f(|l-k+n-m|)}\\&\qquad+\exp[f(|m|)+f(|n|)+f(|l-k|)+f(|l-k+n|)\\&\qquad+f(|k-l+m|)+f(|k-l-n+m|)],\end{aligned}\tag{A17}$$

with $f(j)=e^{-\kappa j\Delta t}\varepsilon^2/\sigma_x^2$. These moments are used in the subsequent calculations of the statistics of the estimators $\hat{C}_x$, $\hat{C}_z$, and $\hat{Z}_{\mathrm{tr}}$.

## APPENDIX B: DETAILED CALCULATION OF Var($\hat{C}_x(n)$)

As described in Sec. III A, the variance of the correlation estimator is expressed in terms of the fourth moment:

$$\begin{aligned}&\mathrm{Var}(\hat{C}_x(n))\\&\quad=\frac{1}{N(N_T-n)^2}\sum_{k,l=0}^{N_T-1-n}\langle x_{i,k}x_{i,k+n}x_{i,l}x_{i,l+n}\rangle\\&\qquad-\frac{1}{N}\{C_x[n\Delta t]\}^2\\&\quad=\frac{1}{N(N_T-n)^2}\sum_{k,l=0}^{N_T-1-n}(\{C_x[n\Delta t]\}^2+\{C_x[(l-k)\Delta t]\}^2\\&\qquad+C_x[(n+l-k)\Delta t]C_x[(n+k-l)\Delta t])\\&\qquad-\frac{1}{N}\{C_x[n\Delta t]\}^2.\end{aligned}\tag{B1}$$

Since the terms in the sum only depend on the difference between the summation indices the following substitution:

$$\sum_{k=0}^{M-1}\sum_{l=0}^{M-1}F(k-l)=\sum_{a=-(M-1)}^{M-1}(M-|a|)F(a)\tag{B2}$$

simplifies the double sum and yields

$$\begin{aligned}&\mathrm{Var}(\hat{C}_x(n))\\&\quad=\frac{1}{N(N_T-n)^2}\sum_{k=-(N_T-n-1)}^{N_T-n-1}(N_T-n-|k|)(\{C_x[k\Delta t]\}^2\\&\qquad+C_x[(n+k)\Delta t]C_x[(n-k)\Delta t]).\end{aligned}\tag{B3}$$

After inserting the correlation function of the Ornstein-Uhlenbeck process, the symmetry of the sum can be used to rewrite the expression as

$$\begin{aligned}&\mathrm{Var}(\hat{C}_x(n))\\&\quad=\frac{\sigma_x^4}{N(N_T-n)^2}\left[2\sum_{a=1}^{N_T-n-1}(N_T-n-a)\left(\mathrm{e}^{-2\kappa a\Delta t}\right.\right.\\&\qquad\left.\left.+\,\mathrm{e}^{-\kappa(|n-a|+n+a)\Delta t}\right)+(N_T-n)\left(\mathrm{e}^{-2\kappa n\Delta t}+1\right)\right],\end{aligned}\tag{B4}$$

where all negative indices are absorbed into the prefactor of the sum and the contribution of the 0th index is appended in the last line. Further simplification is possible after splitting the sum into two sums with fewer terms, i.e., with $1\leqslant a\leqslant n-1$ and $n\leqslant a\leqslant N_T-n-1$, respectively. This step is only correct under the condition $n\leqslant(N_T-1)/2$. Otherwise, the splitting index $n$ would be larger than the final index of the original sum. For both sums the term $\exp[-\kappa(|n-a|+n+a)\Delta t]$ can then be expressed without an absolute value. The new expression reads

$$\begin{aligned}\mathrm{Var}(\hat{C}_x(n)) = \frac{\sigma_x^4}{N(N_T-n)^2}\Bigg[ & 2\sum_{a=1}^{N_T-n-1}(N_T-n-a)\mathrm{e}^{-2\kappa a\Delta t} \\ & + 2\sum_{a=1}^{n-1}(N_T-n-a)\mathrm{e}^{-2\kappa n\Delta t} \\ & + 2\sum_{a=n}^{N_T-n-1}(N_T-n-a)\mathrm{e}^{-2\kappa a\Delta t} \\ & + (N_T-n)\big(\mathrm{e}^{-2\kappa n\Delta t}+1\big)\Bigg]. \end{aligned} \tag{B5}$$

This result is also only correct for $n \geqslant 2$ due to the start and stop indices of the second sum. Thus, $n = 0$ and $n = 1$ have to be treated separately, which, however, yields the same final expression for the variance of the correlation estimator. After rewriting all three sums according to the scheme

$$\sum_{a=k}^{M} h(a) = \sum_{a=0}^{M} h(a) - \sum_{a=0}^{k-1} h(a),$$

with corresponding expressions for $h(a)$, $M$, and $k$, it is possible to identify finite arithmetic and arithmetico-geometric sums for which the following relations exist [31] (Secs. 4.2.1 and 4.2.3 therein):

$$\sum_{n=0}^{M-1}(b+n\cdot c) = \frac{M}{2}[2b+(M-1)c], \tag{B6}$$

$$\sum_{n=0}^{M-1}(b+n\cdot c)r^n = \frac{b-[b+(M-1)c]r^M}{1-r} + \frac{rc(1-r^{M-1})}{(1-r)^2}. \tag{B7}$$

These relations are inserted, and some additional simplifications can be done. The final expression, which holds true for $n \leqslant (N_T-1)/2$, reads

$$\begin{aligned}\mathrm{Var}\big(\hat{C}_x(n)\big) &= \frac{\sigma_x^4}{N(N_T-n)^2}\Bigg\{(N_T-n)(-r^n-1+2r^n n) - r^n(n-1)n \\ &+ \frac{2}{(1-r)^2}[(N_T-n)(1-r) - r + 2r^{N_T-n+1} \\ &+ (N_T-2n)r^n - (N_T-2n+1)r^{n+1}]\Bigg\}, \end{aligned} \tag{B8}$$

where $r \equiv \mathrm{e}^{-2\kappa\Delta t}$. In Ref. [17], an approximate expression for the variance of the correlation estimator of the autoregressive process AR(1),

$$\tilde{x}_{j+1} = \rho\tilde{x}_j + \varepsilon_{j+1}, \tag{B9}$$

is given. Under the assumption $|\rho| < 1$ the correlation reads ([18], p. 81 therein)

$$C_{\tilde{x}}(n) = \sigma_\varepsilon^2\frac{\rho^{|n|}}{1-\rho^2}, \tag{B10}$$

where $\sigma_\varepsilon$ is the standard deviation of the driving noise. This can be simplified using $\langle x_j^2\rangle = 1$ and thus $C_{\tilde{x}}(n) = \rho^{|n|}$. Using this expression, it can be identified that Ref. [17] refers to the correlation estimator defined in Eq. (9) ($n$ in Ref. [17] is identified as $N_T - n$) for the simplified case of a single trajectory, i.e., $N = 1$. Including only the first order in $1/(N_T-n)$ and restricting the result to time indices $n \ll N_T - n$, the variance of the estimator is stated as [17]

$$\mathrm{Var}(\hat{C}_{\tilde{x}}(n)) \sim \frac{1}{N_T-n}\Bigg\{\frac{(1+\rho^2)(1-\rho^{2n})}{1-\rho^2} + \rho^{2n}\bigg[2n + \frac{(\gamma+2)(1+\rho^2)}{1-\rho^2}\bigg]\Bigg\}, \tag{B11}$$

with $\gamma = \langle\tilde{x}^4\rangle - 3$. If the increments $\varepsilon_j$ are Gaussian, also $x$ is Gaussian [16] and due to Wick's theorem $\gamma = 0$. The above expression can be rewritten in terms of the correlation function of the process

$$\mathrm{Var}(\hat{C}_{\tilde{x}}(n)) = \frac{1}{N_T-n}\bigg[\frac{1+\hat{C}_{\tilde{x}}(2)+\hat{C}_{\tilde{x}}(2n)+\hat{C}_{\tilde{x}}(2n+2)}{1-\hat{C}_{\tilde{x}}(2)} + 2n\,\hat{C}_{\tilde{x}}(2n)\bigg] + O\Bigg[\bigg(\frac{1}{N_T-n}\bigg)^2\Bigg]. \tag{B12}$$

Since the AR(1) process can be understood as a temporally discrete version of the Ornstein-Uhlenbeck process [16], the above expression can be compared to our result Eq. (B8). To this end, the parameters in Eq. (B8) are set to $N = 1$ and $\sigma_x^2 = 1$, and all terms of order $O(1/(N_T-n)^2)$ are dropped. This is done under the assumption $n \ll N_T - n$, i.e., in particular, $n^2/(N_T-n)^2 \approx 0$. With these approximations, Eq. (B8) yields

$$\begin{aligned}\mathrm{Var}(\hat{C}_x(n)) &\approx \frac{1}{N_T-n}\bigg[-r^n - 1 + 2r^n n + 2\frac{1-r+r^n-r^{n+1}}{(1-r)^2}\bigg] \\ &= \frac{1}{N_T-n}\bigg[2r^n n + \frac{1+r+r^n+r^{n+1}}{1-r}\bigg] \\ &= \frac{1}{N_T-n}\bigg[\frac{1+C_x(2\Delta t)+C_x(2n\Delta t)+C_x(2(n+1)\Delta t)}{1-C_x(2\Delta t)} \\ &\quad + 2nC_x(2n\Delta t)\bigg]. \end{aligned} \tag{B13}$$

In the second step, the expression is simplified and then rewritten in terms of the exact correlation function of the Ornstein-Uhlenbeck process. This result is equivalent to the result from Ref. [17] up to the difference between the correlation functions of the Ornstein-Uhlenbeck process and the AR(1) process.

### APPENDIX C: DETAILED CALCULATION OF $\mathrm{Cov}(\hat{C}_z(n), \hat{C}_z(m))$ AND $\mathrm{Cov}(\hat{Z}_{\mathrm{tr}}(n), \hat{Z}_{\mathrm{tr}}(m))$

As stated in Sec. III B, the covariance of the correlation estimator is written in terms of the fourth moment

$$\mathrm{Cov}(\hat{C}_z(n), \hat{C}_z(m)) = \frac{1}{N}\left\{\left[\frac{1}{(N_T-n)(N_T-m)}\sum_{l=0}^{N_T-1-n}\sum_{k=0}^{N_T-1-m}\langle z_{i,l}z_{i,l+n}z_{i,k}z_{i,k+m}\rangle\right] - C_z(n\Delta t)C_z(m\Delta t)\right\}. \tag{C1}$$

The fourth moment Eq. (A17) can be inserted. Some terms can be pulled out of the double sum since they do not depend on the summation indices. The remaining terms depend only on the difference between the time indices and not on the absolute terms, i.e., the indices $k$ and $l$ do not appear individually but only as $a \equiv l - k$. Therefore, the double sum over $k$ and $l$ can be simplified with the relation

$$\begin{aligned}\sum_{l=0}^{N_T-1-n}\sum_{k=0}^{N_T-1-m} F(l-k) &= \sum_{a=-N_T+m+1}^{-1}(N_T-m+a)F(a) + \sum_{a=0}^{m-n}(N_T-m)F(a) + \sum_{a=m-n+1}^{N_T-n-1}(N_T-n-a)F(a).\\ &\equiv \left(\sum_{a=-N_T+m+1}^{-1}(N_T-m+a) + \sum_{a=0}^{m-n}(N_T-m) + \sum_{a=m-n+1}^{N_T-n-1}(N_T-n-a)\right)F(a),\end{aligned} \tag{C2}$$

which holds true for $n \leqslant m$. The last step introduces a shorthand notation. This change of summation yields

$$\begin{aligned}\mathrm{Cov}(\hat{C}_z(n), \hat{C}_z(m)) = \frac{1}{N}\Bigg[&-C_z(n\Delta t)C_z(m\Delta t) - 3 + e^{f(|n|)} + e^{f(|m|)} + \frac{1}{(N_T-n)(N_T-m)}\left(\sum_{a=-N_T+m+1}^{-1}(N_T-m+a)\right.\\ &\left.+\sum_{a=0}^{m-n}(N_T-m) + \sum_{a=m-n+1}^{N_T-n-1}(N_T-n-a)\right)\left(e^{f(|a|)} + e^{f(|n+a|)} + e^{f(|m-a|)}\right.\\ &+ e^{f(|m-a-n|)} - e^{f(|m|)+f(|a|)+f(|m-a|)} - e^{f(|n|)+f(|a|)+f(|n+a|)} - e^{f(|m|)+f(|n+a|)+f(|m-n-a|)}\\ &\left.- e^{f(|n|)+f(|m-a|)+f(|m-n-a|)} + e^{f(|m|)+f(|n|)+f(|a|)+f(|n+a|)+f(|m-a|)+f(|a+n-m|)}\right)\Bigg].\end{aligned} \tag{C3}$$

The first line can be expressed in terms of the correlation function and some of the absolute values are irrelevant. The final expression for the covariance reads

$$\begin{aligned}\mathrm{Cov}(\hat{C}_z(n), \hat{C}_z(m)) = &-\frac{[C_z(n\Delta t)-1][C_z(m\Delta t)-1]}{N} + \frac{1}{N(N_T-n)(N_T-m)}\left(\sum_{a=-N_T+m+1}^{-1}(N_T-m+a)\right.\\ &\left.+\sum_{a=0}^{m-n}(N_T-m) + \sum_{a=m-n+1}^{N_T-n-1}(N_T-n-a)\right)\left(e^{f(|a|)} + e^{f(|n+a|)} + e^{f(|m-a|)} + e^{f(|m-a-n|)}\right.\\ &- e^{f(m)+f(|a|)+f(|m-a|)} - e^{f(n)+f(|a|)+f(|n+a|)} - e^{f(m)+f(|n+a|)+f(|m-n-a|)}\\ &\left.- e^{f(n)+f(|m-a|)+f(|m-n-a|)} + e^{f(m)+f(n)+f(|a|)+f(|n+a|)+f(|m-a|)+f(|a+n-m|)}\right).\end{aligned} \tag{C4}$$

As stated above, this result holds true for $n \leqslant m$. The variance can be read by setting $m = n$. In this case, the three sums can be subsumed into one sum, which is symmetric in the summation index. By exploiting this symmetry, Eq. (21) is derived.

In the case of the mean estimator $\hat{Z}_{\mathrm{tr}}(n)$, the covariance is found by inserting the moments from Appendix A into Eq. (24):

$$\begin{aligned}\mathrm{Cov}\big(\hat{Z}_{\mathrm{tr}}(n), \hat{Z}_{\mathrm{tr}}(m)\big) &= \frac{1}{N}\big[e^{f(n)+f(m)+f(|m-n|)} - e^{f(n)} - e^{f(m)} + 1 - (e^{f(n)}-1)(e^{f(m)}-1)\big]\\ &= \frac{1}{N}e^{f(n)+f(m)}\big[e^{f(|m-n|)} - 1\big].\end{aligned} \tag{C5}$$

### APPENDIX D: DETAILED CALCULATION OF $\mathrm{Var}(d)$

The deviation measure $d$ is rewritten in a centered expression, see Eq. (35). To this end, an expression that corresponds to zero is added, i.e.,

$$0 = \langle \hat{C}_z(n)\rangle - \langle \hat{Z}_{\mathrm{tr}}(n)\rangle; \tag{D1}$$

see Eq. (2). This results in

$$
\begin{aligned}
d &\equiv \frac{1}{f}\sum_{n=0}^{n_c}[\hat{Z}_{\mathrm{tr}}(n)-\hat{C}_z(n)]^2\\
&=\frac{1}{f}\sum_{n=0}^{n_c}[\hat{Z}_{\mathrm{tr}}(n)-\langle\hat{Z}_{\mathrm{tr}}(n)\rangle-(\hat{C}_z(n)-\langle\hat{C}_z(n)\rangle)]^2\\
&=\frac{1}{f}\sum_{n=0}^{n_c}\left[\hat{C}_z^{*2}(n)+\hat{Z}_{\mathrm{tr}}^{*2}(n)-2\hat{C}_z^{*}(n)\hat{Z}_{\mathrm{tr}}^{*}(n)\right],
\end{aligned}
\tag{D2}
$$

where $\hat{C}_z^*(n)\equiv\hat{C}_z(n)-\langle\hat{C}_z(n)\rangle$ and $\hat{Z}_{\mathrm{tr}}^*(n)\equiv\hat{Z}_{\mathrm{tr}}(n)-\langle\hat{Z}_{\mathrm{tr}}(n)\rangle$ are introduced. The variance of $d$ is given by

$$
\begin{aligned}
\mathrm{Var}(d)=\langle d^2\rangle-\langle d\rangle^2=\frac{1}{f^2}\sum_{n,m=0}^{n_c}&\big\{\langle\hat{C}_z^{*2}(n)\hat{C}_z^{*2}(m)\rangle+\langle\hat{Z}_{\mathrm{tr}}^{*2}(n)\hat{Z}_{\mathrm{tr}}^{*2}(m)\rangle\\
&+4\langle\hat{C}_z^{*}(n)\hat{Z}_{\mathrm{tr}}^{*}(n)\hat{C}_z^{*}(m)\hat{Z}_{\mathrm{tr}}^{*}(m)\rangle+2\langle\hat{C}_z^{*2}(n)\hat{Z}_{\mathrm{tr}}^{*2}(m)\rangle-4\langle\hat{C}_z^{*2}(n)\hat{C}_z^{*}(m)\hat{Z}_{\mathrm{tr}}^{*}(m)\rangle-4\langle\hat{Z}_{\mathrm{tr}}^{*2}(n)\hat{C}_z^{*}(m)\hat{Z}_{\mathrm{tr}}^{*}(m)\rangle\\
&-\left[\langle\hat{Z}_{\mathrm{tr}}^{*2}(n)\rangle+\langle\hat{C}_z^{*2}(n)\rangle\right]\left[\langle\hat{Z}_{\mathrm{tr}}^{*2}(m)\rangle+\langle\hat{C}_z^{*2}(m)\rangle\right]\big\}.
\end{aligned}
\tag{D3}
$$

As discussed above, the estimators $\hat{C}_z^*$ and $\hat{Z}_{\mathrm{tr}}^*$ are uncorrelated due to the large time lag between the relevant sections of the trajectories. The same argument can be applied to powers of these estimators. As a consequence, all mixed moments factorize into moments of $\hat{C}_z^*$ and moments of $\hat{Z}_{\mathrm{tr}}^*$. Thus,

$$
\begin{aligned}
\mathrm{Var}(d)=\frac{1}{f^2}\sum_{n,m=0}^{n_c}&\big\{\langle\hat{C}_z^{*2}(n)\hat{C}_z^{*2}(m)\rangle+\langle\hat{Z}_{\mathrm{tr}}^{*2}(n)\hat{Z}_{\mathrm{tr}}^{*2}(m)\rangle+4\langle\hat{C}_z^{*}(n)\hat{C}_z^{*}(m)\rangle\langle\hat{Z}_{\mathrm{tr}}^{*}(n)\hat{Z}_{\mathrm{tr}}^{*}(m)\rangle+2\langle\hat{C}_z^{*2}(n)\rangle\langle\hat{Z}_{\mathrm{tr}}^{*2}(m)\rangle\\
&-4\langle\hat{C}_z^{*2}(n)\hat{C}_z^{*}(m)\rangle\langle\hat{Z}_{\mathrm{tr}}^{*}(m)\rangle-4\langle\hat{Z}_{\mathrm{tr}}^{*2}(n)\hat{Z}_{\mathrm{tr}}^{*}(m)\rangle\langle\hat{C}_z^{*}(m)\rangle-\left[\langle\hat{Z}_{\mathrm{tr}}^{*2}(n)\rangle+\langle\hat{C}_z^{*2}(n)\rangle\right]\left[\langle\hat{Z}_{\mathrm{tr}}^{*2}(m)\rangle+\langle\hat{C}_z^{*2}(m)\rangle\right]\big\}.
\end{aligned}
\tag{D4}
$$

As discussed in Sec. III D, a normal distribution of the estimators can be used as an approximation. The application of Wick's theorem results in

$$
\begin{aligned}
\mathrm{Var}(d)&=\frac{1}{f^2}\sum_{n,m=0}^{n_c}\big\{\langle\hat{C}_z^{*2}(n)\rangle\langle\hat{C}_z^{*2}(m)\rangle+2\langle\hat{C}_z^{*}(n)\hat{C}_z^{*}(m)\rangle^2+\langle\hat{Z}_{\mathrm{tr}}^{*2}(n)\rangle\langle\hat{Z}_{\mathrm{tr}}^{*2}(m)\rangle+2\langle\hat{Z}_{\mathrm{tr}}^{*}(n)\hat{Z}_{\mathrm{tr}}^{*}(m)\rangle^2\\
&\quad+4\langle\hat{C}_z^{*}(n)\hat{C}_z^{*}(m)\rangle\langle\hat{Z}_{\mathrm{tr}}^{*}(n)\hat{Z}_{\mathrm{tr}}^{*}(m)\rangle+2\langle\hat{C}_z^{*2}(n)\rangle\langle\hat{Z}_{\mathrm{tr}}^{*2}(m)\rangle-\left[\langle\hat{Z}_{\mathrm{tr}}^{*2}(n)\rangle+\langle\hat{C}_z^{*2}(n)\rangle\right]\left[\langle\hat{Z}_{\mathrm{tr}}^{*2}(m)\rangle+\langle\hat{C}_z^{*2}(m)\rangle\right]\big\}\\
&=\frac{2}{f^2}\sum_{n,m=0}^{n_c}[\langle\hat{C}_z^{*}(n)\hat{C}_z^{*}(m)\rangle+\langle\hat{Z}_{\mathrm{tr}}^{*}(n)\hat{Z}_{\mathrm{tr}}^{*}(m)\rangle]^2\\
&=\frac{2}{f^2}\sum_{n,m=0}^{n_c}[\mathrm{Covar}(\hat{C}_z(n)\hat{C}_z(m))+\mathrm{Covar}(\hat{Z}_{\mathrm{tr}}(n),\hat{Z}_{\mathrm{tr}}(m))]^2.
\end{aligned}
\tag{D5}
$$

Due to the symmetry of the sum, the number of terms in the sum can be reduced, which finally results in Eq. (37).

## APPENDIX E: MODEL OF DISTRIBUTION TAIL

The model distribution of the random variable $c\equiv\hat{C}_z(0)$ consists of the measured histogram $p_{\mathrm{hist}}(c)$ at $c<c_0$ and a tail $p(c)\sim\beta c^{-\alpha}$ at $c\geqslant c_0$. The cutoff point is roughly determined by visual inspection of the measured distribution in Fig. 15 as $c_0=15$. The normalization of this distribution is imposed via

$$
\begin{aligned}
1&=\int_0^{c_0}p_{\mathrm{hist}}(c)\mathrm{d}c+\int_{c_0}^{\infty}\beta c^{-\alpha}\mathrm{d}c\\
&=0.717+\frac{\beta}{\alpha-1}15^{-\alpha+1},
\end{aligned}
\tag{E1}
$$

where the integration interval $c\in[0,\infty)$ is split up and the first integral over the histogram is replaced by the measured value. The condition of a correct mean and variance are translated into conditions for the first and second moments. The latter condition reads

$$\int_0^\infty c^2\, p(c)\mathrm{d}c \;=\int_0^{c_0} c^2\, p_{\mathrm{hist}}(c)\mathrm{d}c\;+\int_{c_0}^\infty \beta c^{-\alpha+2}\mathrm{d}c$$

$$1400.002 = 79.491 + \frac{\beta}{\alpha-3}15^{-\alpha+3}, \tag{E2}$$

where the correct value for the second moment on the left-hand side is obtained from the prediction of $\mathrm{Var}(\hat{C}_z(0))$ and $\langle \hat{C}_z(0)\rangle$. The first term on the right-hand side is measured with the histogram in Fig. 15. These conditions for the correct normalization and second moment are used to determine the parameters of the tail as $\alpha = 3.10133$ and $\beta = 176.048$ by solving the system of equations in Mathematica [32]. The mean of this the model distribution can be calculated as

$$\int_0^\infty c\, p(c)\mathrm{d}c = \int_0^{c_0} c\, p_{\mathrm{hist}}(c)\mathrm{d}c\;+\int_{c_0}^\infty \beta c^{-\alpha+1}\mathrm{d}c = 7.346 + \frac{\beta}{\alpha-2}15^{-\alpha+2}, \tag{E3}$$

where the measured value for the first integral is inserted in the second line. Inserting the model parameters leads to $\langle \hat{C}_z(0)\rangle = 15.445$, which is close to the predicted mean of the estimator at $\langle \hat{C}_z(0)\rangle = 14.643$. The resulting variance of the model distribution is $\mathrm{Var}(\hat{C}_z(0)) = 1161.376$, which is approximately equivalent to the predicted value of $\mathrm{Var}(c) = 1185.595$. Hence, the model distribution has a correct normalization and is approximately consistent with the predicted values for the mean and variance.


[1] H. Risken, *The Fokker-Planck Equation*, 2nd ed. (Springer, Berlin, 1989).

[2] N. G. van Kampen, *Stochastic Processes in Physics and Chemistry*, Revised and Enlarged ed. (North-Holland, Amsterdam, 1992).

[3] C. W. Gardiner, *Handbook of Stochastic Methods*, 2nd ed. (Springer-Verlag, Berlin, 1985).

[4] K. Engbring, D. Boriskovsky, Y. Roichman, and B. Lindner., A nonlinear fluctuation-dissipation test for Markovian systems, Phys. Rev. X **13**, 021034 (2023).

[5] L. Willareth, I. M. Sokolov, Y. Roichman, and B. Lindner, Generalized fluctuation-dissipation theorem as a test of the Markovianity of a system, Europhys. Lett. **118**, 20001 (2017).

[6] R. Satija, A. M. Berezhkovskii, and D. E. Makarov, Broad distributions of transition-path times are fingerprints of multidimensionality of the underlying free energy landscapes, Proc. Natl. Acad. Sci. USA **117**, 27116 (2020).

[7] R. Zwanzig, *Nonequilibrium Statistical Mechanics* (Oxford University Press, Oxford, 2001).

[8] A. Lapolla and A. Godec, Manifestations of projection-induced memory: General theory and the tilted single file, Front. Phys. **7**, 182 (2019).

[9] L. Onsager and S. Machlup, Fluctuations and irreversible processes, Phys. Rev. **91**, 1505 (1953).

[10] A. Lapolla and A. Godec, Toolbox for quantifying memory in dynamics along reaction coordinates, Phys. Rev. Res. **3**, L022018 (2021).

[11] A. M. Berezhkovskii and D. E. Makarov, Single-molecule test for Markovianity of the dynamics along a reaction coordinate, J. Phys. Chem. Lett. **9**, 2190 (2018).

[12] K. Song, D. E. Makarov, and E. Vouga, Compression algorithms reveal memory effects and static disorder in single-molecule trajectories, Phys. Rev. Res. **5**, L012026 (2023).

[13] L. Dinis, P. Martin, J. Barral, J. Prost, and J. F. Joanny, Fluctuation-response theorem for the active noisy oscillator of the hair-cell bundle, Phys. Rev. Lett. **109**, 160602 (2012).

[14] G. Gradziuk, G. Torregrosa, and C. P. Broedersz, Irreversibility in linear systems with colored noise, Phys. Rev. E **105**, 024118 (2022).

[15] S. Thapa, D. Zaretzky, R. Vatash, G. Gradziuk, C. Broedersz, Y. Shokef, and Y. Roichman, Nonequilibrium probability currents in optically-driven colloidal suspensions, SciPost Phys. **17**, 096 (2024).

[16] J. Honerkamp, *Stochastic Dynamical Systems. Concepts, Numerical Methods, Data Analysis* (Wiley/VCH, Weinheim, 1993).

[17] M. S. Bartlett, On the theoretical specification and sampling properties of autocorrelated time-series, Supplement to the J. R. Stat. Soc. **8**, 27 (1946).

[18] P. J. Brockwell and R. A. Davis, *Time Series: Theory and Methods*, 2nd ed., Springer Series in Statistics (Springer, New York, 1991).

[19] K. Neusser, *Time Series Econometrics*, Springer Texts in Business and Economics (Springer, Bern, 2016).

[20] M. S. Fadali, *Introduction to Random Signals, Estimation Theory, and Kalman Filtering* (Springer, Singapore, 2024).

[21] K. Weise and W. Wöger, *Meßunsicherheit und Meßdatenauswertung* (Wiley-VCH, Weinheim, 1999).

[22] C. Gardiner, *Elements of Stochastic Methods* (AIP Publishing, Melville, 2021).

[23] M. A. Pinsky and S. Karlin, *An Introduction to Stochastic Modeling*, 4th ed. (Academic Press, Burlington, 2011).

[24] R. Goerlich, B. Sorkin, D. Boriskovsky, L. B. Pires, B. Lindner, C. Genet, and Y. Roichman, Consistent thermodynamics reconstructed from transitions between nonequilibrium steady-states, arXiv:2601.03245.

[25] R. Goerlich, A. Tartar, Y. Roichman, and I. M. Sokolov, Fluctuation-response relation for a nonequilibrium system with resolved Markovian embedding, arXiv:2601.05198.

[26] G. Podhaisky, I. M. Sokolov, Y. Roichman, and B. Lindner, Markov test reliability, Zenodo (2025), https://doi.org/10.5281/zenodo.19349444.

[27] R. A. Maller, G. Müller, and A. Szimayer, Ornstein-Uhlenbeck processes and extensions, in *Handbook of Financial Time Series*, edited by T. G. Andersen, R. A. Davis, J.-P. Kreiß, and T. Mikosch (Springer, Berlin, 2009), pp. 421–437.

[28] A. G. Cherstvy, S. Thapa, Y. Mardoukhi, A. V. Chechkin, and R. Metzler, Time averages and their statistical variation for the Ornstein-Uhlenbeck process: Role of initial particle distributions and relaxation to stationarity, Phys. Rev. E **98**, 022134 (2018).

[29] R. L. Stratonovich, *Topics in the Theory of Random Noise. Volume I*, Mathematics and its Applications (Gordon and Breach, New York, 1963), Vol. 3.

[30] G. Skoulakis, A recursive formula for computing central moments of a multivariate lognormal distribution, Am. Stat. **62**, 147 (2008).

[31] K. F. Riley, M. P. Hobson, and S. J. Bence, *Mathematical Methods for Physics and Engineering. A Comprehensive Guide*, 2nd ed. (Cambridge University Press, Cambridge, 2002).

[32] Wolfram Research, Inc., Mathematica, Version 14.2, Champaign, IL (2025).